

# Hastatic Order in URu<sub>2</sub>Si<sub>2</sub>

Premala Chandra<sup>1</sup>, Piers Coleman<sup>1,3</sup>, and Rebecca Flint<sup>2</sup>

<sup>1</sup>*Center for Materials Theory, Department of Physics and Astronomy,  
Rutgers University, 136 Frelinghuysen Rd., Piscataway, NJ 08854-8019, USA*

<sup>2</sup>*Department of Physics, Massachusetts Institute for Technology,  
Massachusetts Avenue, Cambridge, MA 02139-4307, USA and*

<sup>3</sup> *Department of Physics, Royal Holloway,  
University of London, Egham, Surrey TW20 0EX, UK.*

(Dated: May 23, 2018)

## Abstract

The development of collective long-range order via phase transitions occurs by the spontaneous breaking of fundamental symmetries. Magnetism is a consequence of broken time-reversal symmetry while superfluidity results from broken gauge invariance. The broken symmetry that develops below 17.5K in the heavy fermion compound URu<sub>2</sub>Si<sub>2</sub> has long eluded such identification. Here we show that the recent observation of Ising quasiparticles in URu<sub>2</sub>Si<sub>2</sub> results from a spinor order parameter that breaks *double* time-reversal symmetry, mixing states of integer and half-integer spin. Such “hastatic order” hybridizes conduction electrons with Ising  $5f^2$  states of the uranium atoms to produce Ising quasiparticles; it accounts for the large entropy of condensation and the magnetic anomaly observed in torque magnetometry. Hastatic order predicts a tiny transverse moment in the conduction sea, a colossal Ising anisotropy in the nonlinear susceptibility anomaly and a resonant energy-dependent nematicity in the tunneling density of states.

The hidden order (HO) that develops below 17.5K in the heavy fermion compound URu<sub>2</sub>Si<sub>2</sub> is particularly notable, having eluded identification for twenty five years[1–13]. Recent spectroscopic[14–18], magnetometric[19] and high-field measurements[20, 21] suggest that the HO is connected with the formation of an itinerant heavy electron fluid, a consequence of quasiparticle hybridization between localized, spin-orbit coupled f-moments and mobile conduction electrons. Though the development of hybridization at low temperatures is usually associated with a crossover, in URu<sub>2</sub>Si<sub>2</sub> both optical [22] and tunnelling [15–17] probes suggest that it develops abruptly at the HO transition, leading to proposals[10, 11] that the hybridization is an order parameter.

High temperature bulk susceptibility measurements on URu<sub>2</sub>Si<sub>2</sub> show that the local 5f moments embedded in the conduction sea are Ising in nature[1, 26], while quantum oscillation (QO) experiments deep within the HO phase reveal that the quasiparticles exhibit a giant Ising anisotropy[21, 23, 24]. The Zeeman splitting depends solely on the c-axis component of the magnetic field,  $\Delta E = g(\theta)\mu_B B$ [24], with a g-factor  $g(\theta) = g \cos \theta$ , where  $\theta$  is the angle relative to the c-axis. The g-factor anisotropy exceeds 30, corresponding to an anisotropy of the Pauli susceptibility in excess of 900; this anisotropy is also observed in the angle-dependence of the Pauli-limited upper critical field of the superconducting state[23, 24], showing that the Ising quasiparticles pair to form a heavy fermion superconductor. This giant anisotropy suggests that the f-moment is transferred to the mobile quasiparticles through hybridization[28]. In the tetragonal crystalline environment of URu<sub>2</sub>Si<sub>2</sub> such Ising anisotropy is only natural in integer spin configurations[4, 27], thus the most likely valence of the *U* ions with an integer spin is a  $5f^2$  configuration. Moreover, the observation of paired Ising quasiparticles in a superconductor with  $T_c \sim 1.5K$  indicates that this  $5f^2$  configuration is degenerate to within an energy resolution of  $g\mu_B H_c \sim 5K$ . In URu<sub>2</sub>Si<sub>2</sub>, tetragonal symmetry protects a magnetic non-Kramers  $\Gamma_5$  doublet, the candidate origin of the Ising quasiparticles[4, 29].

The quasiparticle hybridization of half-integer spin conduction electrons with an integer spin doublet in URu<sub>2</sub>Si<sub>2</sub> has profound implications for hidden order; such mixing can not occur without broken *double* time-reversal symmetry. Time-reversal,  $\hat{\Theta}$ , is an anti-unitary quantum operator with *no* associated quantum number[30]. However double-reversal  $\hat{\Theta}^2$ , equivalent to a  $2\pi$  rotation, forms a unitary operator with an associated quantum number, the “Kramers index”  $K$ [30]. The Kramers index,  $K = (-1)^{2J}$  of a quantum state of to-

tal angular momentum  $J$  defines the phase factor acquired by its wavefunction after two successive time-reversals,  $\hat{\Theta}^2|\psi\rangle = K|\psi\rangle = |\psi^{2\pi}\rangle$ . An integer spin state  $|\alpha\rangle$  is unchanged by a  $2\pi$  rotation, so  $|\alpha^{2\pi}\rangle = +|\alpha\rangle$  and  $K = 1$ . However, conduction electrons with half-integer spin states,  $|\mathbf{k}\sigma\rangle$ , where  $\mathbf{k}$  is momentum and  $\sigma$  is the spin component, change sign,  $|\mathbf{k}\sigma^{2\pi}\rangle = -|\mathbf{k}\sigma\rangle$ , so  $K = -1$ .

While conventional magnetism breaks time-reversal symmetry, it is invariant under  $\hat{\Theta}^2$  so the Kramers index is conserved. However in URu<sub>2</sub>Si<sub>2</sub>, the hybridization between integer and half-integer spin states requires a quasiparticle mixing term of the form  $\mathcal{H} = (|\mathbf{k}\sigma\rangle V_{\sigma\alpha}(\mathbf{k})\langle\alpha| + \text{H.c.})$  in the low energy fixed point Hamiltonian. After two successive time-reversals

$$|\mathbf{k}\sigma\rangle V_{\sigma\alpha}(\mathbf{k})\langle\alpha| \rightarrow |\mathbf{k}\sigma^{2\pi}\rangle V_{\sigma\alpha}^{2\pi}(\mathbf{k})\langle\alpha^{2\pi}| = -|\mathbf{k}\sigma\rangle V_{\sigma\alpha}^{2\pi}(\mathbf{k})\langle\alpha|. \quad (1)$$

Since the microscopic Hamiltonian is time-reversal invariant, it follows that  $V_{\sigma\alpha}(\mathbf{k}) = -V_{\sigma\alpha}^{2\pi}(\mathbf{k})$ ; the hybridization thus breaks time-reversal symmetry in a fundamentally new way, forming an order parameter that, like a spinor, reverses under  $2\pi$  rotations. The resulting ‘‘hastatic (Latin: *spear*) order’’, is a state of matter that breaks both single and double time-reversal symmetry and is thus distinct from conventional magnetism.

Indirect support for time-reversal symmetry-breaking in the hidden order phase of URu<sub>2</sub>Si<sub>2</sub> is provided by recent magnetometry measurements that indicate the development of an anisotropic basal-plane spin susceptibility,  $\chi_{xy}$ , at the hidden order transition[19].  $\chi_{xy}$  is a conduction electron response to scattering off the hidden order (c.f. Fig. 2.), leading to a scattering matrix of the form  $t(\mathbf{k}) = (\sigma_x + \sigma_y)d(\mathbf{k})$ , where  $d(\mathbf{k})$  is the scattering amplitude.  $t(\mathbf{k})$  has been linked to a spin nematic state[12], under the special condition that  $d(-\mathbf{k}) = -d^*(\mathbf{k})$  to avoid time-reversal symmetry breaking. However, if the scattering process involves resonant hybridization in the f-channel, then  $d(\mathbf{k})$  is associated with resonant scattering off the f-state, a process with a real, even parity scattering amplitude,  $d(\mathbf{k}) = d(-\mathbf{k})$ . In this case, the observed t-matrix is necessarily odd under time-reversal in the hidden order phase.

Hybridization in heavy fermion compounds is usually driven by valence fluctuations mixing a ground-state Kramers doublet and an excited singlet (cf. Fig. 1a). In this case, the hybridization amplitude is a scalar that develops via a crossover, leading to mobile heavy fermions. However valence fluctuations from a  $5f^2$  ground-state create excited states with

an odd number of electrons and hence a Kramers degeneracy (cf. Fig. 1b). Then the quasi-particle hybridization has two components,  $\Psi_\sigma$ , that determine the mixing of the excited Kramers doublet into the ground-state. These two amplitudes form a spinor defining the “hastatic” order parameter

$$\Psi = \begin{pmatrix} \Psi_\uparrow \\ \Psi_\downarrow \end{pmatrix}. \quad (2)$$

The presence of distinct up/down hybridization components indicates that  $\Psi$  carries the global spin quantum number; its development must now break double time-reversal and spin rotational invariance via a phase transition.

Under pressure, URu<sub>2</sub>Si<sub>2</sub> undergoes a first-order phase transition from the hidden order (HO) state to an antiferromagnet (AFM) [31]. These two states are remarkably close in energy and share many key features[20, 32, 33] including common Fermi surface pockets; this motivated the recent proposal that despite the first order transition separating the two phases, they are linked by “adiabatic continuity,”[32] corresponding to a notional rotation of the HO in internal parameter space [5, 34]. In the magnetic phase, this spinor points along the c-axis

$$\Psi_A \sim \begin{pmatrix} 1 \\ 0 \end{pmatrix}, \Psi_B \sim \begin{pmatrix} 0 \\ 1 \end{pmatrix} \quad (3)$$

corresponding to time-reversed configurations on alternating layers A and B, leading to a large staggered Ising moment. For the HO state, the spinor points in the basal plane

$$\Psi_A \sim \frac{1}{\sqrt{2}} \begin{pmatrix} e^{-i\phi/2} \\ e^{i\phi/2} \end{pmatrix}, \Psi_B \sim \frac{1}{\sqrt{2}} \begin{pmatrix} -e^{-i\phi/2} \\ e^{i\phi/2} \end{pmatrix}, \quad (4)$$

where again,  $\Psi_B = \Theta\Psi_A$  and it is protected from developing a large moment by the pure Ising character of the  $5f^2$  ground-state.

Hastatic order permits a direct realization of the adiabatic continuity between the HO and AFM in terms of a single Landau functional for the free energy

$$f[T, P, B_z] = [\alpha(T_c - T) - \eta_z B_z^2]|\Psi|^2 + \beta|\Psi|^4 - \gamma(\Psi^\dagger \sigma_z \Psi)^2 \quad (5)$$

where  $\gamma = \delta(P - P_c)$  is a pressure-tuned anisotropy term. The unique feature of the theory is that the non-Kramers doublet has Ising character, and only couples to the z-component of the magnetic field  $B_z = B \cos \theta$ . The resulting Ising splitting of the non-Kramer’s doublet

suppresses the Kondo effect, giving rise to the  $B_z^2$  term in the quadratic coefficient, where the coefficient  $\eta_z$  is of order  $1/T_{HO}^2$ . [35] The phase diagram predicted by this free energy is shown in Fig. 1 (c). When  $P < P_c(T)$ , the vector  $\Psi^\dagger \vec{\sigma} \Psi = |\Psi|^2(n_x, n_y, 0)$  lies in the basal plane, resulting in hastatic order. At  $P = P_c$ , there is a first order “spin-flop” into an magnetic state where  $\Psi^\dagger \vec{\sigma} \Psi = |\Psi|^2(0, 0, \pm 1)$  lies along the c-axis.

Adiabatic continuity provides a natural interpretation of the soft longitudinal spin fluctuations observed to develop in the HO state [36] as an incipient Goldstone excitation between the two phases [34]. In the HO state, rotations between hastatic and AFM order will lead to a gapped Ising collective mode which we identify with the longitudinal spin fluctuations observed in inelastic neutron scattering [36]. At the first order line,  $P = P_c$ , the quartic anisotropy term vanishes; we predict that the gap to longitudinal spin fluctuations will soften according to  $\Delta \propto \sqrt{\gamma|\Psi|^2} \sim |\Psi|\sqrt{P_c(T) - P}$  (see Supplementary material). Experimental observation of this feature would provide confirmation of the common origin of the hidden and AFM order.

Another prediction of the phenomenological theory is the development of a nonlinear susceptibility anomaly with a colossal Ising anisotropy. From the Landau theory[35], the jump in the specific heat  $\Delta C$ , the susceptibility and nonlinear susceptibility anomalies  $d\chi_1/dT$  and  $\Delta\chi_3$  obey the relation  $\frac{\Delta C}{T_c} \Delta\chi_3 = 12 \left(\frac{d\chi_1}{dT}\right)^2$ , where  $\frac{d\chi_1}{dT} = -\frac{\alpha}{2\beta} \eta_z \cos^2 \theta$ , so that  $\chi_3 \propto \cos^4 \theta$ . A large anomaly in the c-axis nonlinear susceptibility of URu<sub>2</sub>Si<sub>2</sub> has been observed at  $T_c$ [25, 26], but its Ising anisotropy has never been quantified. The predicted development of a colossal Ising anisotropy in the zero-field non-linear susceptibility at the hidden order transition is another consequence of hastatic order.

We now present a model that relates hastatic order to the valence fluctuations in URu<sub>2</sub>Si<sub>2</sub>, based on a two-channel Anderson lattice model. The uranium ground-state is a  $5f^2$  Ising  $\Gamma_5$  doublet[4],  $|\pm\rangle = a|\pm 3\rangle + b|\mp 1\rangle$ , written in terms of  $J = 5/2$  f-electrons in the three tetragonal orbitals  $\Gamma_7^\pm$  and  $\Gamma_6$

$$\begin{aligned} |+\rangle &= (af_{\Gamma_7^\downarrow}^\dagger f_{\Gamma_7^\downarrow}^\dagger + bf_{\Gamma_6^\uparrow}^\dagger f_{\Gamma_7^\uparrow}^\dagger)|0\rangle \\ |-\rangle &= (af_{\Gamma_7^\uparrow}^\dagger f_{\Gamma_7^\uparrow}^\dagger + bf_{\Gamma_6^\downarrow}^\dagger f_{\Gamma_7^\downarrow}^\dagger)|0\rangle. \end{aligned} \quad (6)$$

The lowest lying excited state is most likely the  $5f^3$  ( $J = 9/2$ ) state, but for simplicity here we take it to be the symmetry-equivalent  $5f^1$  state. Valence fluctuations from the ground state ( $5f^2 \Gamma_5$ ) to the excited state ( $5f^1 \Gamma_7^\pm$ ) occur in two orthogonal conduction

channels,[37, 38]  $\Gamma_7^-$  and  $\Gamma_6$ . This allows us to read off the hybridization matrix elements of the Anderson model

$$H_{VF}(j) = V_6 c_{\Gamma_6\pm}^\dagger(j) |\Gamma_7^\pm\rangle \langle \Gamma_5 \pm | + V_7 c_{\Gamma_7\mp}^\dagger(j) |\Gamma_7^\mp\rangle \langle \Gamma_5 \pm | + \text{H.c.} \quad (7)$$

where  $\pm$  denotes the ‘‘up’’ and ‘‘down’’ states of the coupled Kramers and non-Kramers doublets. The field  $c_{\Gamma\sigma}^\dagger(j) = \sum_{\mathbf{k}} \left[ \Phi_{\Gamma}^\dagger(\mathbf{k}) \right]_{\sigma\tau} c_{\mathbf{k}\tau}^\dagger e^{-i\mathbf{k}\cdot\mathbf{R}_j}$  creates a conduction electron at site  $j$  with spin  $\sigma$  in a Wannier orbital with symmetry  $\Gamma \in \{6, 7\}$ , while  $V_6$  and  $V_7$  are the corresponding hybridization strengths. The full model is then written

$$H = \sum_{\mathbf{k}\sigma} \epsilon_{\mathbf{k}} c_{\mathbf{k}\sigma}^\dagger c_{\mathbf{k}\sigma} + \sum_j [H_{VF}(j) + H_a(j)] \quad (8)$$

while  $H_a(j) = \Delta E \sum_{\pm} |\Gamma_7^\pm, j\rangle \langle \Gamma_7^\pm, j|$  is the atomic Hamiltonian.

Hastatic order is revealed by factorizing the Hubbard operators,  $|\Gamma_7^\pm\rangle \langle \Gamma_5\alpha| = \hat{\Psi}_\sigma^\dagger \chi_\alpha$ . Here  $|\Gamma_5\alpha\rangle = \chi_\alpha^\dagger |\Omega\rangle$  is the non-Kramers doublet, represented by the pseudo-fermion  $\chi_\alpha^\dagger$ , while  $\hat{\Psi}_\sigma^\dagger$  is a slave boson[39] representing the excited  $f^1$  doublet  $|\Gamma_7^\pm\rangle = \hat{\Psi}_\sigma^\dagger |\Omega\rangle$ . Hastatic order is the condensation of this boson  $\Psi_\sigma^\dagger \chi_\alpha \rightarrow \langle \hat{\Psi}_\sigma \rangle \chi_\alpha$ , generating a hybridization between the conduction electrons and the Ising  $5f^2$  state while also breaking double time reversal. The  $\Gamma_5$  doublet has both magnetic and quadrupolar moments represented by  $\chi^\dagger \vec{\sigma} \chi = (\mathcal{O}_{x^2-y^2}, \mathcal{O}_{xy}, m^z)$ , where  $m^z$  is the Ising magnetic moment and  $\mathcal{O}_{x^2-y^2}$  and  $\mathcal{O}_{xy}$  are quadrupole moments. The tensor product  $Q_{\alpha\beta} \equiv \Psi_\alpha \Psi_\beta^\dagger$  describes the development of composite order between the non-Kramers doublet and the spin density of conduction electrons. Composite order has been considered by several earlier authors in the context of two channel Kondo lattices[37, 42, 43] in which the valence fluctuations have been integrated out. However, by factorizing the composite order in terms of the spinor  $\Psi_\alpha$ , we are able to directly understand the development of coherent Ising quasiparticles and the broken double time-reversal.

Using this factorization, we can rewrite the valence fluctuation term as,

$$H_{VF}(j) = \sum_{\mathbf{k}} c_{\mathbf{k}\sigma}^\dagger \hat{\mathcal{V}}_{\sigma\eta}(\mathbf{k}, j) \chi_\eta(j) e^{-i\mathbf{k}\cdot\mathbf{R}_j} + \text{H.c.} \quad (9)$$

where  $\hat{\mathcal{V}}(\mathbf{k}, j) = V_6 \Phi_{\Gamma_6}^\dagger(\mathbf{k}) \hat{B}_j^\dagger + V_7 \Phi_{\Gamma_7}^\dagger(\mathbf{k}) \hat{B}_j^\dagger \sigma_1$ ,  $\hat{B}_j = \begin{pmatrix} \hat{\Psi}_\uparrow & 0 \\ 0 & \hat{\Psi}_\downarrow \end{pmatrix}$ . In the ordered state,

$B_j = \langle \hat{B}_j \rangle$  is replaced by its expectation value, so that in the HO state

$$\langle B_j^\dagger \rangle = |\Psi| \begin{pmatrix} e^{i(\mathbf{Q}\cdot\mathbf{R}_j+\phi)/2} & 0 \\ 0 & e^{-i(\mathbf{Q}\cdot\mathbf{R}_j+\phi)/2} \end{pmatrix} \equiv |\Psi|U_j, \quad (10)$$

with magnitude  $|\Psi|$ . The internal angle,  $\phi$ , rotates  $B_j$  within the basal plane.

As the HO and AFM appear to share a single commensurate wavevector,  $\mathbf{Q} = (0, 0, \frac{2\pi}{c})$ [20, 32, 33], we use this wavevector here. It is convenient to absorb the unitary matrix,  $U_j$  into the pseudo-fermion,  $\tilde{\chi}_j = U_j\chi_j$ . This gauge transformation transfers the charge from the slave boson to the pseudo-fermion, making it a charged quasiparticle. In this gauge, one channel ( $\Gamma_6$ ) is uniform, while the other ( $\Gamma_7^-$ ) is staggered

$$H_{VF} = \sum_{\mathbf{k}} c_{\mathbf{k}}^\dagger \mathcal{V}_6(\mathbf{k})\chi_{\mathbf{k}} + c_{\mathbf{k}}^\dagger \mathcal{V}_7(\mathbf{k})\chi_{\mathbf{k}+\mathbf{Q}} + \text{h.c.} \quad (11)$$

where the hybridization form factors  $\mathcal{V}_7(\mathbf{k}) = V_7\Phi_7^\dagger(\mathbf{k})\sigma_1$  and  $\mathcal{V}_6(\mathbf{k}) = V_6\Phi_6^\dagger(\mathbf{k})$ .

There are two general aspects of this condensation that deserve special comment. First, the two-channel Anderson impurity model is known to possess a non-Fermi liquid ground-state with an entanglement entropy of  $\frac{1}{2}k_B \ln 2$ [40]. The development of hastatic order liberates this zero-point entropy, accounting naturally for the large entropy of condensation. As a slave boson,  $\Psi$  carries both the charge  $e$  of the electrons and the local gauge charge  $Q_j = \Psi_j^\dagger\Psi_j + \chi_j^\dagger\chi_j$  of constrained valence fluctuations, its condensation gives a mass to their relative phase via the Higg's mechanism[41]. But as a Schwinger boson, the condensation of  $\Psi$  this process breaks the SU(2) spin symmetry. In this way the hastatic boson can be regarded as a magnetic analog of the Higg's boson.

One of the key elements of the hastatic theory is the formation of mobile Ising quasiparticles, and the observed Ising anisotropy enables us to set some of the parameters of the theory. The full anisotropic g-factor is a combination of f-electron and conduction electron components given by  $g(\theta) \approx g^* \cos \theta + g_c \left(\frac{T_K}{D}\right)$  where  $g_c = 2$  and the factor  $T_K/D$  derives from the small conduction electron admixture in the quasiparticles. Experimentally[21], the g-factor anisotropy is in excess of 30, i.e.  $g_z/g_\perp \sim D/T_K \gtrsim 30$ , which enables us to phenomenologically set a lower bound on  $D/T_K$  in our model. The g-factor is defined in terms of the Zeeman splitting of the heavy fermion dispersion,  $\Delta E_{\mathbf{k}\eta} = |E_{\mathbf{k}\eta\uparrow} - E_{\mathbf{k}\eta\downarrow}| = g_{\mathbf{k}\eta}(\theta)\mu_B B$ , where  $\eta \in [1, 4]$  is a band-index. Fig. 3(a) shows the Fermi surface averaged g-factor, defined

by

$$\overline{g(\theta)} = \frac{\sum_{\mathbf{k}\eta} g_{\mathbf{k}\eta}(\theta)\delta(E_{\mathbf{k}\eta})}{\sum_{\mathbf{k}\eta} \delta(E_{\mathbf{k}\eta})} \quad (12)$$

calculated within the mean-field hastatic model, as a function of field angle to the c-axis, choosing the lower-bound estimate  $D/T_K \sim 30$ .

Another key aspect of the hastatic picture is that there must be time-reversal symmetry breaking in both the HO and AFM phases, manifested by a staggered moment; in the AFM this leads to a large c-axis f-electron moment, but in the HO it becomes a small transverse moment carried by conduction electrons,  $\vec{m}_c = -g\mu_B \text{Tr} \vec{\sigma} \mathcal{G}^c(\mathbf{k}, \mathbf{k} + \mathbf{Q})$ , where  $\mathcal{G}^c$  is the conduction electron Green's function[35]. The small magnitude of the induced moment is a consequence of the Clogston-Anderson compensation theorem that states that changes in the conduction electron magnetization are set by the same ratio  $T_K/D$  that determines the g-factor anisotropy[44]. There will also be a small mixed-valent contribution from the excited Kramers doublet,  $\vec{m}_1 \propto \langle \Psi^\dagger \vec{\sigma} \Psi \rangle$ . The angle of the moments in the plane is controlled by the internal hastatic angle,  $\phi$ . Fig. (3b) shows the temperature dependence of the magnetic moment calculated for a case where  $D/T_K \approx 30$ , for which  $m_\perp(0) = 0.015\mu_B$ , which is an upper bound for the predicted conduction electron moment. Neutron scattering measurements on URu<sub>2</sub>Si<sub>2</sub> have placed bounds on the c-axis magnetization of the f-electrons using a momentum transfer  $Q$  in the basal plane. Detection of an  $m_\perp(0)$  carried by conduction electrons, with a small scattering form-factor, will require high-resolution measurements with a c-axis momentum transfer. We note that there have been reports from  $\mu$ SR and NMR measurements[45, 46] of very small intrinsic basal plane fields in URu<sub>2</sub>Si<sub>2</sub>, which are consistent with this theory.

Although the conduction electrons develop a magnetic moment, the non-Kramers  $5f^2$  state carries no dipolar or quadrupolar moment,  $\langle \chi^\dagger \vec{\sigma} \chi \rangle = 0$ . In the microscopic model the quadrupolar moments vanish because of the d-wave form factor between the  $\Gamma_6$  and  $\Gamma_7$ -channels[35]. The absence of a charge quadrupole implies there will be no lattice distortion associated with hastatic order. By contrast, hastatic order does induce a weak broken tetragonal symmetry in the spin channel. In the HO state, the inter-channel components of the hastatic t-matrix,  $\hat{\mathcal{V}}_6 \hat{\mathcal{V}}_7^\dagger \propto \sigma_x + \sigma_y$ , break tetragonal symmetry in the spin channel, resulting in a nonzero spin susceptibility within the conduction fluid,

$$\chi_{xy} = -(g\mu_B)^2 \text{Tr} \sigma_x \mathcal{G}^c(\mathbf{k}, \mathbf{k} + \mathbf{Q}) \sigma_y \mathcal{G}^c(\mathbf{k} + \mathbf{Q}, \mathbf{k}) \propto (\text{Tr} \hat{\mathcal{V}}_6 \hat{\mathcal{V}}_7^\dagger)^2 \quad (13)$$



of a magnitude of order  $(\frac{T_K}{D})^2$ , that onsets at the hidden order temperature as  $|\Psi|^4 \sim (T_c - T)^2$  as shown in Fig. (3c).

Hastatic order also manifests itself as an anisotropic hybridization gap, which vanishes along lines in momentum space, giving rise to a “V”-shaped density of states due to the partial gapping of the Fermi surface, as shown in Fig (4), which will be smeared out by disorder in the real material. The anisotropy of the hybridization also breaks tetragonal symmetry, giving rise to a energy dependent nematicity  $\eta(E)$  that peaks over a narrow energy window around the f-resonance. Some of this nematicity is present at the Fermi surface, accounting for the splitting seen in quantum oscillation frequencies[47] and cyclotron resonance experiments[48]. An ideal way to verify this prediction is via scanning tunneling spectroscopy (STS), where the measured differential conductivity,  $dI/dV \propto A(eV, \vec{x})$  is proportional to the local density of states  $A(eV, \vec{x})$  at position  $\vec{x}$  on the surface. A measure of the broken tetragonal symmetry is provided by the “nematicity”

$$\eta(V) = \frac{\overline{\frac{dI}{dV}(x, y) \text{sign}(x - y)}}{\left(\overline{\left(\frac{dI}{dV}\right)^2} - \left(\overline{\frac{dI}{dV}}\right)^2\right)^{\frac{1}{2}}}. \quad (14)$$

Here  $(x, y)$  is the co-ordinate relative to the center of the unit cell and the overbar denotes an average over the unit cell. The resonant scattering of the hastatic order causes this quantity to vary rapidly as a function of voltage, over an energy range of order the Kondo temperature  $T_K$ . Fig. (4) shows the variation of the nematicity, calculated within our model of hastatic order. As one passes through the Kondo resonance, this quantity is found to change sign, and to peak at a maximum value of approximately 50%.

So far we have focused on the mean field consequences of hastatic order. The recently observed softening of the commensurate longitudinal spin fluctuations at  $T_c$ [49] suggests that hastatic order melts via phase fluctuations. While the hybridization spinor itself,  $\langle \Psi \rangle$ , can only become nonzero below the phase transition at  $T_c$ , we expect that its amplitude,  $\langle \Psi^\dagger \Psi \rangle$ , will persist to higher temperatures. As  $\langle \Psi^\dagger \vec{\sigma} \Psi \rangle$  remains zero above  $T_c$ , only the non-symmetry breaking (uniform, intrachannel) components of the hybridization can develop:  $\hat{\mathcal{V}}_6 \hat{\mathcal{V}}_6^\dagger$  and  $\hat{\mathcal{V}}_7 \hat{\mathcal{V}}_7^\dagger$  will emerge via a crossover at a higher temperature  $T^*$  to create an incoherent Fermi liquid, consistent with the heavy mass inferred from thermodynamic and optical measurements[1, 18] and the development of Fano signatures in both scanning and point-contact tunneling spectroscopy[15–17]. The symmetry-breaking, interchannel components,

$\hat{\mathcal{V}}_6\sigma_1\hat{\mathcal{V}}_7^\dagger$  will always develop precisely at the HO transition. Another aspect of experiments that is not covered by our mean field description, is the observation of gapped, low-energy incommensurate fluctuations around a Q-vector  $Q^* = (1 \pm 0.4, 0, 0)$  in the hidden order phase, which appears to be a sign of an unfulfilled predisposition towards an incommensurate phase, probably driven by partial Fermi surface nesting. These effects lie beyond a mean-field description, but would emerge from the Gaussian fluctuations about the mean-field theory .

Though we have discussed hastatic order in the context of URu<sub>2</sub>Si<sub>2</sub>, it should be a more a widespread phenomenon associated with hybridization in any f-electron material whose unfilled f-shell contains a geometrically-stabilized non-Kramers doublet. As such, we expect realizations of hastatic order in other 5f uranium and 4f praseodymium intermetallics.

- 
- [1] T.T.M. Palstra et al., “Superconducting and Magnetic Transitions in the Heavy-Fermion System  $URu_2Si_2$ ,” *Phys. Rev. Lett.* **55** 2727 (1985).
  - [2] W. Schlabitz et al., J. Baumann, B. Pollit, U. Rauchschwalbe, H.M. Mayer, U. Ahlheim and C.D. Bredl, “Superconductivity and Magnetic Order in a Strongly Interacting Fermi System: URu<sub>2</sub>Si<sub>2</sub> ”, *Z. Phys. B.*, 62, 171-177 (1986).
  - [3] J. A. Mydosh and P. M. Oppeneer, “Colloquium: Hidden Order, Superconductivity and Magnetism – The Unsolved Case of URu<sub>2</sub>Si<sub>2</sub> ”, *Rev. Mod. Physics*, in press (2011).
  - [4] H. Amitsuka and T. Sakakibara, “Single Uranium-Site Properties of the Dilute Heavy Electron System  $U_xTh_{1-x}Ru_2Si_2$  ( $x \leq 0.07$ ),” *J. Phys. Soc. Japan* **63** 736 (1994).
  - [5] K. Haule and G. Kotliar, “Arrested Kondo Effect and Hidden Order in  $URu_2Si_2$ ,” *Nature Phys.* **5**, 796 (2009).
  - [6] P. Santini and G. Amoretti, “Crystal Field Model of the Magnetic Properties of URu<sub>2</sub>Si<sub>2</sub>”, *Physical Review Letters* **73**, 1027 (1994).
  - [7] P. Chandra, P. Coleman, J. A. Mydosh and V. Tripathi, “Hidden orbital order in the heavy fermion URu<sub>2</sub>Si<sub>2</sub> ”, *Nature* 417, 831, 2002.
  - [8] C. M. Varma and L. Zhu, “Helicity Order: Hidden Order Parameter in URu<sub>2</sub>Si<sub>2</sub> ”, *Phys. Rev. Lett.* 96, 036405 (2006).
  - [9] C. Pépin, M. R. Norman, S. Burdin, and A. Ferraz, ”Modulated Spin Liquid: A New Paradigm

- for  $URu_2Si_2$ ”, *Phys. Rev. Lett.* **106**, 106601 (2011).
- [10] Ting Yuan, Jeremy Figgins and Dirk K. Morr, “Hidden Order Transition in  $URu_2Si_2$  and the Emergence of a Coherent Kondo Lattice”, arXiv:1101.2636v1 (2011).
- [11] Y. Dubi and A.V. Balatsky, “Hybridization Wave as the ‘Hidden Order’ in  $URu_2Si_2$ ”, *Phys. Rev. Lett.* **106**, 08640 (2011).
- [12] S. Fujimoto, “Spin Nematic State as a Candidate of the Hidden Order Phase of  $URu_2Si_2$ ”, *Phys. Rev. Lett.* **106**, 196407 (2011).
- [13] H. Ikeda et al, “Emergent Rank-5 ‘Nematic’ Order in  $URuSi_2$ ”, preprint (2011).
- [14] A. F. Santander-Syro et al., “Fermi-surface instability at the ‘hidden order’ transition of  $URu_2Si_2$ ” *Nature Physics* **5**, 637 - 641 (2009).
- [15] A. R. Schmidt et al., “Atomic-Scale Electronic Structure of a Kondo-Hole in a Heavy Fermion Metal”, *Nature* **465**, 570 (2010).
- [16] P. Aynajian et al., “Visualizing the Formation of the Kondo Lattice and the Hidden Order in  $URu_2Si_2$ ”, *PNAS* **107**, 10 383 (2010).
- [17] W.K. Park et al, “Fano Resonance and Hybridization Gap in Kondo Lattice  $URu_2Si_2$ ”, unpublished (2011).
- [18] U. Nagel et al., “The normal state of  $URu_2Si_2$ : Spectroscopic Evidence for an Anomalous Fermi Liquid”, to be published (arXiv:1107.5574v1)..
- [19] R. Okazaki et al., “Rotational Symmetry Breaking in the Hidden Order Phase of  $URu_2Si_2$ ”, *Science* **331** 439 (2011).
- [20] E. Hassinger et al, “Similarity of the Fermi Surface in the Hidden Order State and in the Antiferromagnetic State of  $URu_2Si_2$ ”, *Phys. Rev. Lett.* **105**, 216409 (2010).
- [21] M.M. Altarawneh et al., “Sequential Spin Polarization of the Fermi Surface Pockets of  $URu_2Si_2$  and its Implications for the Hidden Order,” *Phys. Rev. Lett.* **106** 146403 (2011).
- [22] D. A. Bonn et al, “Far-Infrared Properties of  $URu_2Si_2$ ”, *Phys. Rev. Lett.*, **61**, 1305 (1988).
- [23] J. P. Brison et al, “Anisotropy of the upper critical field in  $URu_2Si_2$  and FFLO state in antiferromagnetic superconductors”, *Physica C* **250**, 128 (1995).
- [24] M. M. Altarawneh et al. , “Superconducting pairs with extreme uniaxial anisotropy in  $URu_2Si_2$ ” *Phys. Rev. Lett.* **108**, 066407 (2012).
- [25] Y. Miyako et al., *J. Appl. Phys.* **70**, 5791 (1991).
- [26] A.P. Ramirez et al., “Nonlinear Susceptibility as a Probe of Tensor Spin Order in  $URu_2Si_2$ ”,

- Phys. Rev. Lett.* **68** 2680 (1992).
- [27] R. Flint, P. Chandra and P. Coleman, “Basal-Plane Nonlinear Susceptibility: A Direct Probe of the Single-Ion Physics in  $URu_2Si_2$ ”, arXiv:1207.2433 (2012).
- [28] E. A. Goremychkin et al., “Magnetic Correlations and the Anisotropic Kondo Effect in  $Ce_{1-x}La_xAl_3$ ”, *Phys. Rev. Lett.* **89**, 147201 (2002).
- [29] F.J. Ohkawa and H. Shimizu, “Quadrupole and Dipole Orders in  $URu_2Si_2$ ,” *J. Phys: Cond. Mat.* **11**, L519 (1999).
- [30] J. J. Sakurai, “Modern Quantum Mechanics”, Revised Edition, pp 277, (Addison-Wesley), (1994).
- [31] H. Amitsuka et al., “Pressure-Temperature Phase Diagram of the Heavy-Electron Superconductor  $URu_2Si_2$ ,” *J. Magn. Magn. Mater.* **310**, 214 (2007).
- [32] Y.J. Jo et al., “Field-Induced Fermi Surface Reconstruction and Adiabatic Continuity between Antiferromagnetism and the Hidden-Order State in  $URu_2Si_2$ ,” *Phys. Rev. Lett.* **98**, 166404 (2007).
- [33] A. Villaume et al., “Signature of Hidden Order in Heavy Fermion Superconductor  $URu_2Si_2$ : Resonance at the wave vector  $Q_0 = (1, 0, 0)$ ,” *Phys. Rev. B* **78** 5114 (2008).
- [34] K. Haule and G. Kotliar, “Complex Landau-Ginzburg Theory of the Hidden Order in  $URu_2Si_2$ ,” *Eur. Lett.* **80** 57006 (2010).
- [35] See supplementary material.
- [36] C. Broholm et al., “Magnetic excitations in the heavy-fermion superconductor  $URu_2Si_2$ ,” *Phys. Rev. B.* **43**, 12809 (1991).
- [37] D.L. Cox and M. Jarrell, “The Two-Channel Kondo route to non-Fermi liquids,” *J. Phys. Cond. Mat.* **8** 9825 (1996).
- [38] D. L. Cox and A. Zawadowski, “Exotic Kondo Effects in Metals”, Taylor & Francis, London. (2002).
- [39] P. Coleman, “A New approach to the Mixed Valence Problem”, *Phys. Rev. B* **28**, 5255 (1983).
- [40] C. Bolech and N. Andrei, “Solution of the Two-Channel Anderson Impurity Model: Implications for the Heavy Fermion  $UBe_{13}$ ”, *Phys. Rev. Lett.*, **88** 2002.
- [41] P. Coleman, J. B. Marston and A. J. Schofield, “Transport anomalies in a simplified model for a heavy-electron quantum critical point, *Phys. Rev.* **72**, 245111 (2003)
- [42] P. Coleman, A. M. Tselik, N. Andrei & H. Y. Kee, *Phys. Rev. B* **60**, 3608(1999).

- [43] S. Hoshino, J. Otsuki and Y. Kuramoto, “Diagonal Composite Order in a Two-Channel Kondo Lattice” *Phys. Rev. Lett.* 107, 247202 (2011).
- [44] P.W. Anderson, “Localized magnetic states in metals”, *Phys. Rev.* 124,41 (1961);P.W. Anderson and A.M. Clogston, *Bull. Am. Phys. Soc.* 6, 124 (1961).
- [45] H. Amitsuka et al., “Inhomogeneous magnetism in URu<sub>2</sub>Si<sub>2</sub> studied by muon spin relaxation under high pressure,” *Physica B* 326, 418-421 (2003).
- [46] O.O. Bernal et al., “Ambient Pressure <sup>99</sup>Ru NMR in *URu<sub>2</sub>Si<sub>2</sub>*: Internal Field Anisotropy,” *J. Mag. Magn. Mat.* **e59-60** 272 (2004).
- [47] H. Okhuni et al., “Fermi surface properties and de Haas-van Alphen oscillation in both the normal and superconducting mixed states of URu<sub>2</sub>Si<sub>2</sub> ”, *Philos. Mag. B* 79, 1045 (1999).
- [48] Private communication from Y. Matsuda (cyclotron resonance)
- [49] P. G. Niklowitz et al., “Role of commensurate and incommensurate low-energy excitations in the paramagnetic to hidden-order transition of URu<sub>2</sub>Si<sub>2</sub> ”, arXiv:1110.5599 (2011).

**Acknowledgments** An early version of this work was begun in collaboration with Patrick Fazekas, since deceased. We thank N. Andrei, S. Burdin, B. Coleman, N. Harrison, K. Haule, G. Kotliar, P. Lee, G. Luke, L. Greene, Y. Matsuda, J. Mydosh, P. Niklowitz, C. Pépin, T. Senthil, A. Toth and T. Timusk for useful discussions. We acknowledge funding from the Simons Foundation (Flint), the National Science Foundation grants DMR 0907179 (Flint, Coleman) and grant 1066293 (Flint, Chandra, Coleman) while at the Aspen Center for Physics. We are grateful for the hospitality of the Aspen Center for Physics.

**Competing Interests** The authors declare that they have no competing financial interests.

**Correspondence** and requests for materials should be addressed to Piers Coleman. (email: coleman@physics.rutgers.edu).

## Figure Captions

**Fig. 1.** (a) A normal Kondo effect occurs in ions with an odd number of f-electrons, where the ground state is guaranteed to be doubly degenerate by time-reversal symmetry (known as a Kramers doublet). Virtual valence fluctuations to an excited singlet state are associated with a scalar hybridization. (b) In URu<sub>2</sub>Si<sub>2</sub>, quasiparticles inherit an Ising symmetry from a  $5f^2$  non-Kramers doublet. Loss or gain of an electron necessarily leads to an excited Kramers doublet, and the development of a coherent hybridization is associated with a two-component spinor hybridization that carries a magnetic quantum number and must therefore develop at a phase transition. (c) Phase diagram for hastatic order, showing how tuning the parameter  $\lambda \propto (P - P_c)$  leads to a spin flop between hastatic order and Ising magnetic order. Inset: at the 1st order line, the longitudinal spin gap is predicted to vanish as  $\Delta \propto \sqrt{P_c - P}$ . (d) Polar plot showing the predicted  $\cos^4 \theta$  form of the non-linear susceptibility  $\chi_3$  induced by hastatic order, where  $\theta$  is the angle of the field from the c-axis.

**Fig. 2.** Phenomenological interpretation of the anomalous spin susceptibility in URu<sub>2</sub>Si<sub>2</sub>. (a) The anomalous spin susceptibility is given by conduction electrons scattering off the hidden order, sandwiched between  $\sigma_x$  and  $\sigma_y$  vertices. (b) The anomalous scattering t-matrix can be rewritten as a resonant scattering off the order parameter.

**Fig. 3.** Magnetic response of hastatic order. (a) Polar plot of calculated g-factor,  $g(\theta)$  averaged over the Fermi surface, as a function of magnetic field angle  $\theta$  (see SOM for details), compared with results of Altarawneh et al. [21], overlaid in green. (b) As a consequence of the broken time-reversal symmetry, we predict a staggered conduction electron moment that onsets at the HO transition with a linear  $T_c - T$  temperature dependence (staggering pattern shown in inset). The magnitude of this moment is governed by  $T_K/D \sim .01\mu_B/U$ . (c) We have calculated the tetragonal symmetry breaking component of the uniform susceptibility,  $\chi_{xy}(T)$ . To compare our results to Okazaki et al[19] (overlaid as green squares), we have plotted the two-fold oscillation amplitude of the magnetic torque,  $A$  (in black), where  $A \cos 2\phi \equiv \frac{\tau_{2\phi}}{V} = -\frac{\mu_0 H^2}{V} \cos 2\phi \chi_{xy}(T)$ .  $A$  goes as  $(T_c - T)^2$  just below the HO transition. For details of our calculation, including parameter choices, please see the supporting online material[35].

**Fig. 4.** Density of states and resonant nematicity predicted by theory. Upper panel: density of states as a function of energy predicted by model calculation (blue line), showing f and conduction electron components. Red line, voltage dependence of nematicity  $\eta(V)$  in model calculation of scanning tunneling spectrum. Lower panels: spatial dependence of density of states for selected bias voltages in model calculation of scanning tunneling spectrum, showing the resonant character of the nematicity.

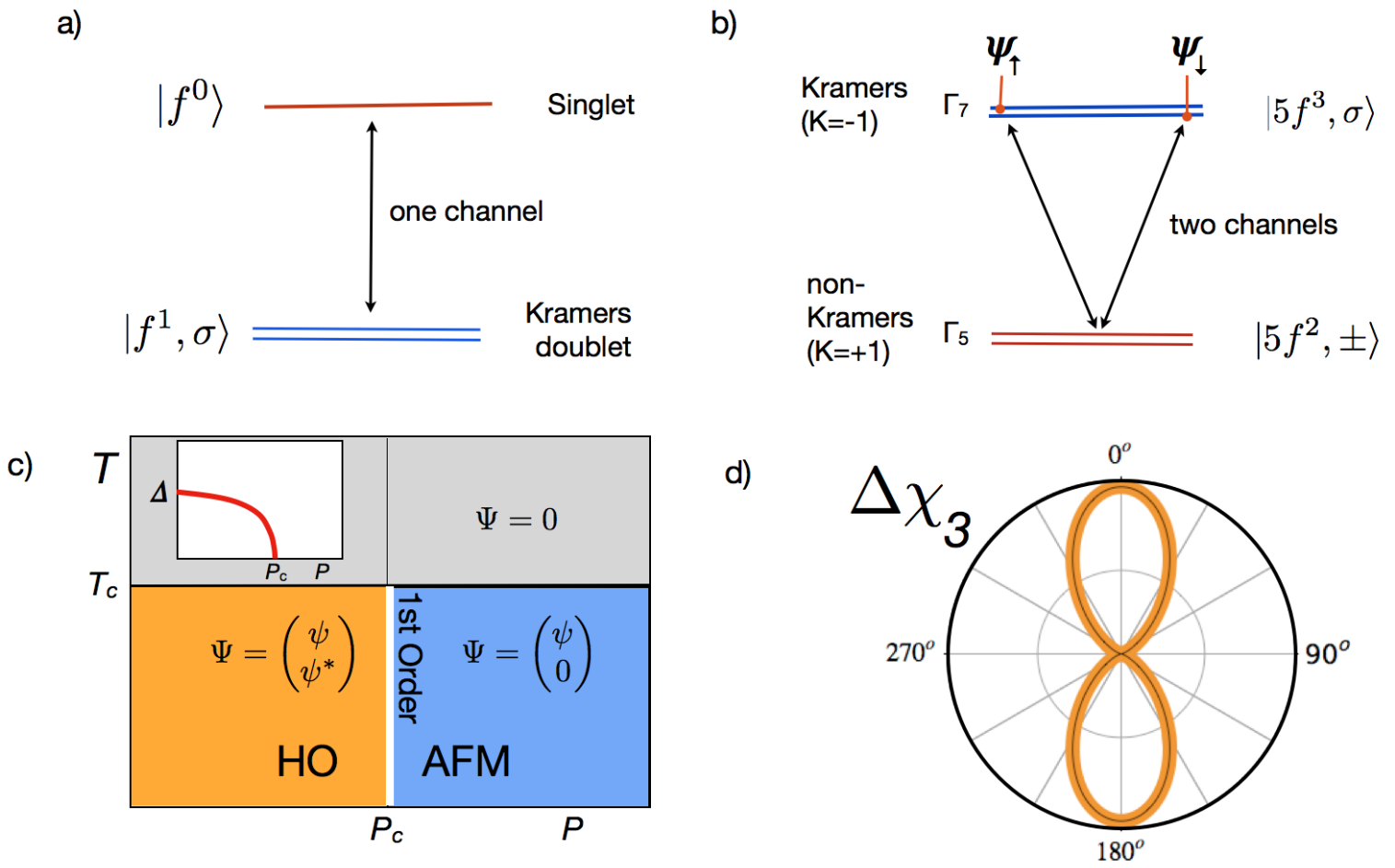
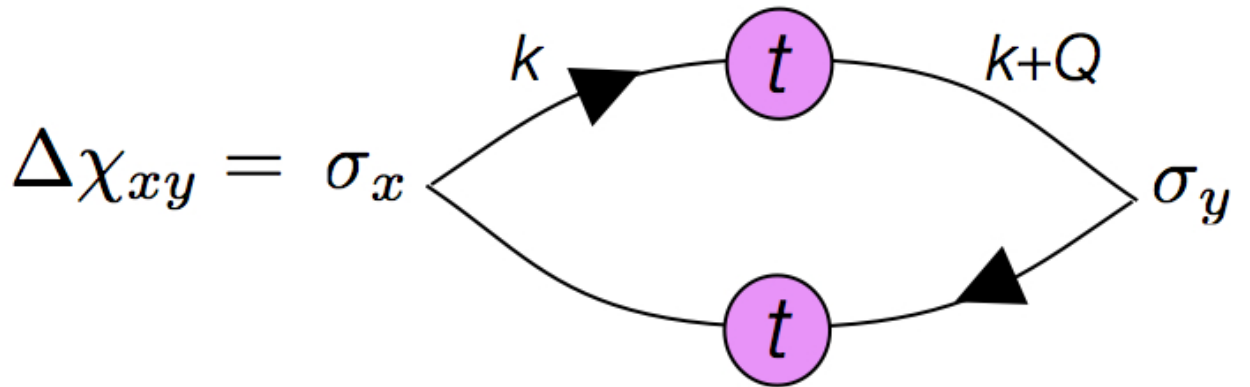


Figure 1.



a)



b)

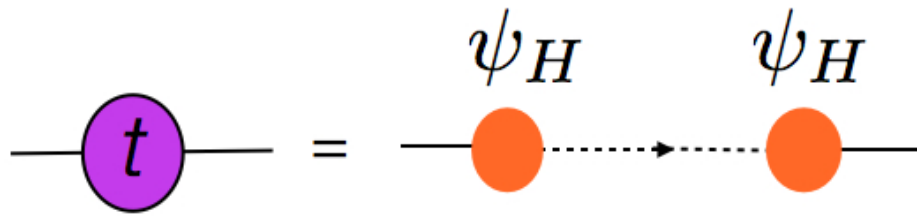


Figure 2.

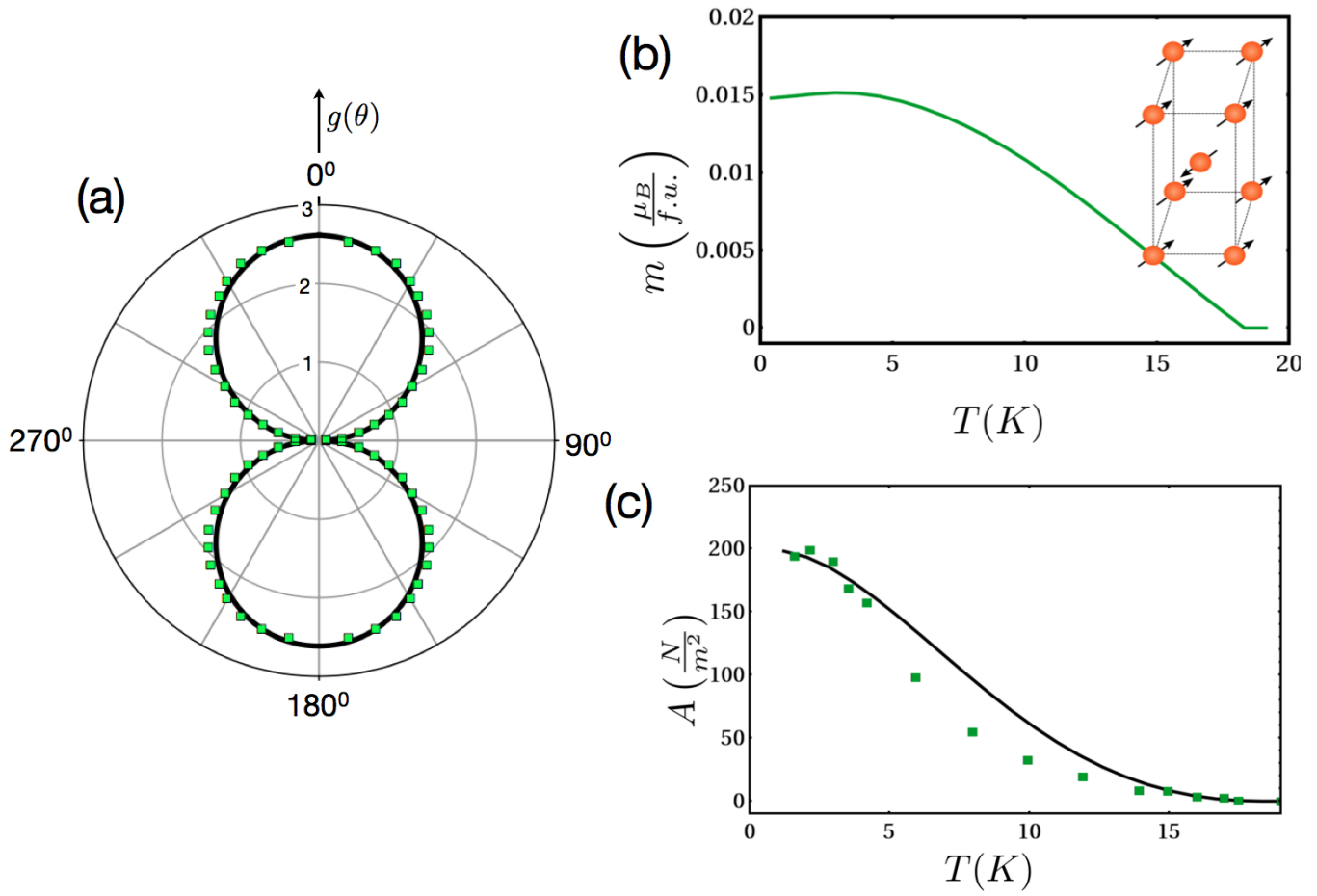


Figure 3.

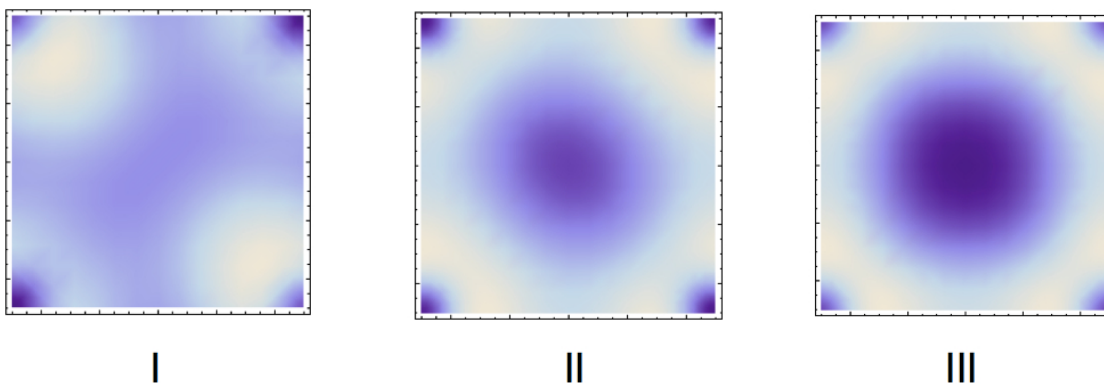
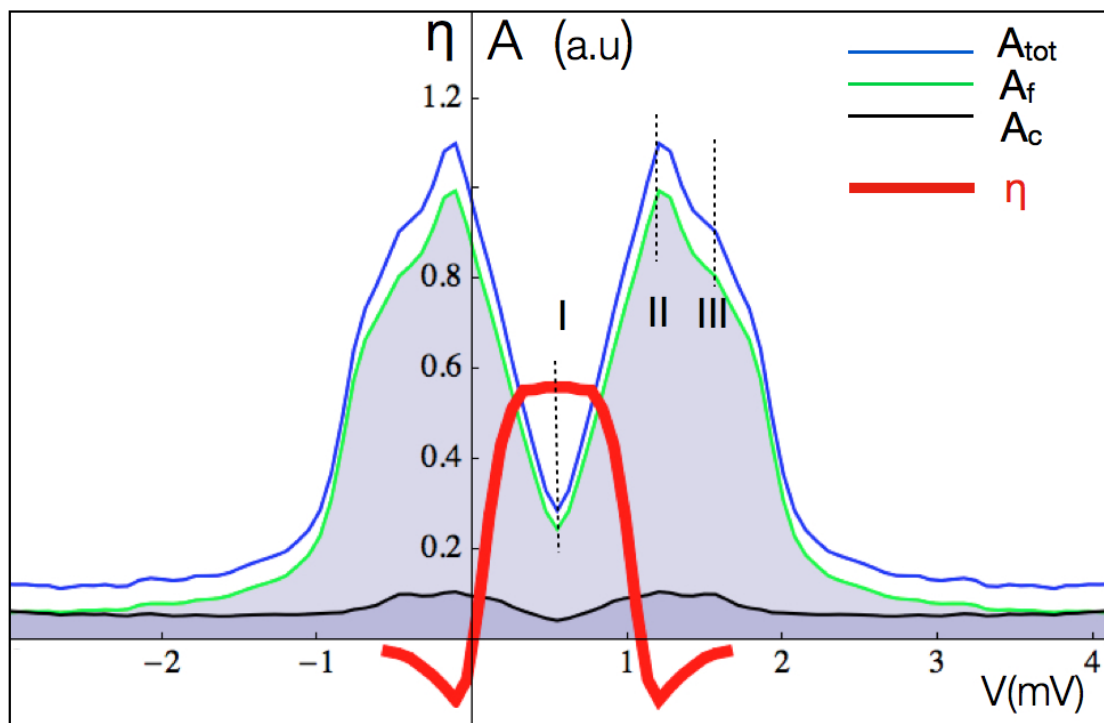


Figure 4.

# Supplementary Information

Online material: **Hastatic order in URu<sub>2</sub>Si<sub>2</sub>**

Premala Chandra<sup>1</sup>, Piers Coleman<sup>1,2</sup> and Rebecca Flint<sup>3</sup>

<sup>1</sup>*Center for Materials Theory, Rutgers University, 136 Frelinghuysen Rd., Piscataway, NJ 08854-8019, USA*

<sup>2</sup>*Department of Physics, Royal Holloway, University of London, Egham, Surrey TW20 0EX, UK.*

<sup>3</sup>*Department of Physics, Massachusetts Institute for Technology, Cambridge, MA 02139-4307, USA*

## CONTENTS

I. Absence of Ising symmetry in a Kramers doublet with Tetragonal Symmetry.	2
II. Estimate of $T_K$ for URu <sub>2</sub> Si <sub>2</sub>	3
III. Landau theory for hastatic order.	3
A. Landau theory in zero field	3
B. Landau Theory in Magnetic Field: Nonlinear Susceptibility	5
1. Estimating $\eta_z$ and $\eta_\perp$	6
IV. Two channel Anderson lattice model for URu <sub>2</sub> Si <sub>2</sub>	8
V. Magnetization and susceptibility calculation	13
VI. Current neutron scattering bounds on the transverse moment	15
VII. Density of states	16
VIII. g-factors	16
IX. Model Tunneling conductance and nematicity calculation	17
References	19

## I. ABSENCE OF ISING SYMMETRY IN A KRAMERS DOUBLET WITH TETRAGONAL SYMMETRY.

A central argument in the main paper is that the Ising symmetry of the quasiparticles in URu<sub>2</sub>Si<sub>2</sub> must derive from a non-Kramers doublet. This section establishes that a Kramers doublet in a tetragonal crystal lacks the selection rules required for an Ising symmetry without fine tuning. A tetragonal crystal field Hamiltonian contains terms of the form  $J_{\pm}^4$  allowed by the four-fold symmetry in the basal plane. These terms cause a pure doublet  $|\pm M\rangle$  (where  $M$  is some  $J_z \in \{-J, \dots, J\}$ ), to mix with states  $|\pm M'\rangle$  differing by four units of angular momentum, where  $M' = M - 4n$ , and  $n$  is any integer. A magnetic doublet in an tetragonal environment thus has the form

$$\begin{aligned} |\Gamma+\rangle &= \sum_n a_n |M - 4n\rangle \\ |\Gamma-\rangle &= \sum_n a_n |-M + 4n\rangle. \end{aligned} \quad (1)$$

The coefficients  $a_n$  may always be chosen to be real. Ising symmetry requires that the matrix elements

$$\langle \Gamma + | J_{\pm} | \Gamma - \rangle = \sum_{n,n'} a_n a_{n'} \langle M - 4n | J_{\pm} | -M + 4n' \rangle \quad (2)$$

vanish. In the absence of fine-tuning ( $a_n = 0$  for all  $n \neq 0$ ), this implies a selection rule  $\langle M - 4n | J_{\pm} | -M + 4n' \rangle = 0$ . Such terms vanish if  $M - 4n \neq -M + 4n' \pm 1$ , or  $M \neq 2(n - n') \pm \frac{1}{2}$ . Since  $n$  and  $n'$  are integers,  $M$  must be an integer. For any half-integer  $M$ , corresponding to a Kramers doublet, the selection rule is absent and the ion will develop a generic basal plane moment. The fine-tuned case will produce an Ising Kramers doublet, but corresponds to the complete absence of tetragonal mixing, highly unlikely in a tetragonal environment. However, for integer  $M$ , corresponding to a non-Kramers doublet, the selection rule  $\langle M - 4n \pm | J_{\pm} | \Gamma - M + 4n' \rangle = 0$  causes every term in the above sum (2) to vanish so the transverse moment is necessarily zero, yielding perfect Ising symmetry.

By contrast, in a hexagonal system like CeAl<sub>3</sub>, the crystal field Hamiltonian contains terms of the form  $J_{\pm}^6$ . Such terms again mix a pure doublet  $|\pm M\rangle$  with terms  $|\pm M'\rangle$ , where  $M' = M - 6n$ , integer  $n$ . However, for  $J < 7/2$ , there are no choices of  $M$  and  $M'$  that differ by 6, and thus there will be two Ising doublets for the Ce,  $J = 5/2$  case:  $\Gamma_8 = |\pm 5/2\rangle$  and  $\Gamma_9 = |\pm 3/2\rangle$ . Either of these Kramers doublets could undergo a *single*

*channel* Ising Kondo effect[9, 17], which will differ substantially from the two-channel Kondo physics associated with a non-Kramers doublet.

## II. ESTIMATE OF $T_K$ FOR URu<sub>2</sub>Si<sub>2</sub>

In our mean field theory, all Kondo behavior develops at the hidden order transition. Incorporating Gaussian fluctuations should suppress the hidden order phase transition,  $T_{HO}$ , while allowing many of the signatures of heavy fermion physics, including the quenching of the spin entropy and the heavy mass to develop at a higher crossover scale,  $T_K$ . While the coherence temperature estimated from the resistivity,  $T^* \approx 70K$  is much larger than the hidden order temperature,  $T_{HO} = 17.5K$ , an entropic estimate of the Kondo temperature,  $S(T_K) = \frac{1}{2}R \log 2$  gives an effective Kondo temperature not much larger than  $T_{HO}$ . There is considerable uncertainty in the entropy associated with the development of hidden order,  $S(T_{HO})$ , due to difficulties subtracting the phonon and other non-electronic contributions, leading to estimates ranging from  $.15R \log 2$ [8] to  $.3R \log 2$ [7]. If we take a conservative estimate of  $S(T_{HO}) = .2R \log 2$ , and the normal state  $\gamma = 180\text{mJ/molK}^2$ [7],  $S(T_K) = .2R \log 2 + \int_{T_{HO}}^{T_K} \gamma dT = \frac{1}{2}R \log 2$  yields  $T_K = 27K$ , much lower than the coherence temperature seen in the resistivity.

## III. LANDAU THEORY FOR HASTATIC ORDER.

### A. Landau theory in zero field

The most general Landau functional for the free energy density of a hastatic state with a spinorial order parameter  $\Psi$  as a function of pressure and temperature is

$$f[\Psi] = \alpha(T_c - T)|\Psi|^2 + \beta|\Psi|^4 - \gamma(\Psi^\dagger \sigma_z \Psi)^2 \quad (4)$$

where  $\gamma = \delta(P - P_c)$  is a pressure-tuned anisotropy term and

$$\Psi = r \begin{pmatrix} \cos(\theta/2)e^{i\phi/2} \\ \sin(\theta/2)e^{-i\phi/2} \end{pmatrix}, \quad (5)$$

where  $\theta$  is the disclination of  $\Psi^\dagger \vec{\sigma} \Psi$  from the c-axis. Using this expression for  $\Psi$ ,

$$f = -\alpha(T - T_c)r^2 + \beta r^4 - \gamma r^4 \cos^2 \theta. \quad (6)$$

If  $P < P_c$ , then  $\gamma < 0$  and the minimum of the free energy occurs for  $\theta = \pi/2$ , corresponding to the hidden order state ordered state. By contrast, if  $P > P_c$ , then  $\gamma > 0$  and the minimum of the free energy occurs at  $\theta = 0, \pi$ , corresponding to the antiferromagnet. The “spin flop” in  $\theta$  at  $P = P_c$  corresponds to a first order phase transition between the hidden order and antiferromagnet (See Fig. 1)

To study the soft modes of the hastatic order, we need to generalize the Landau theory to a time-dependent Landau Ginzburg theory for the action, with action  $S = \int L dt d^3x$ , where the Lagrangian

$$-L[\Psi] = f[\Psi] + \rho \left( |\nabla\Psi|^2 - c^{-2}|\dot{\Psi}|^2 \right),$$

and  $\rho$  is the stiffness. Expanding  $\Psi$  around its equilibrium value  $\Psi_0$ , taking  $\phi = 0$  for convenience and writing

$$\Psi(x, t) = \Psi_0 e^{i\delta\theta(x)\sigma_y/2} = (1 + i/2 \sum_q \delta\theta(q) e^{i\vec{q}\cdot\vec{x} - \omega t} \sigma_y) \Psi_0. \quad (7)$$

This gives rise to a change in  $\Psi^\dagger \sigma_z \Psi = \hat{x}|\Psi_0|^2 + \delta\theta(x)\hat{z}|\Psi_0|^2$  corresponding to a fluctuation in the longitudinal magnetization. This rotation in  $\Psi$  does not affect the first two isotropic

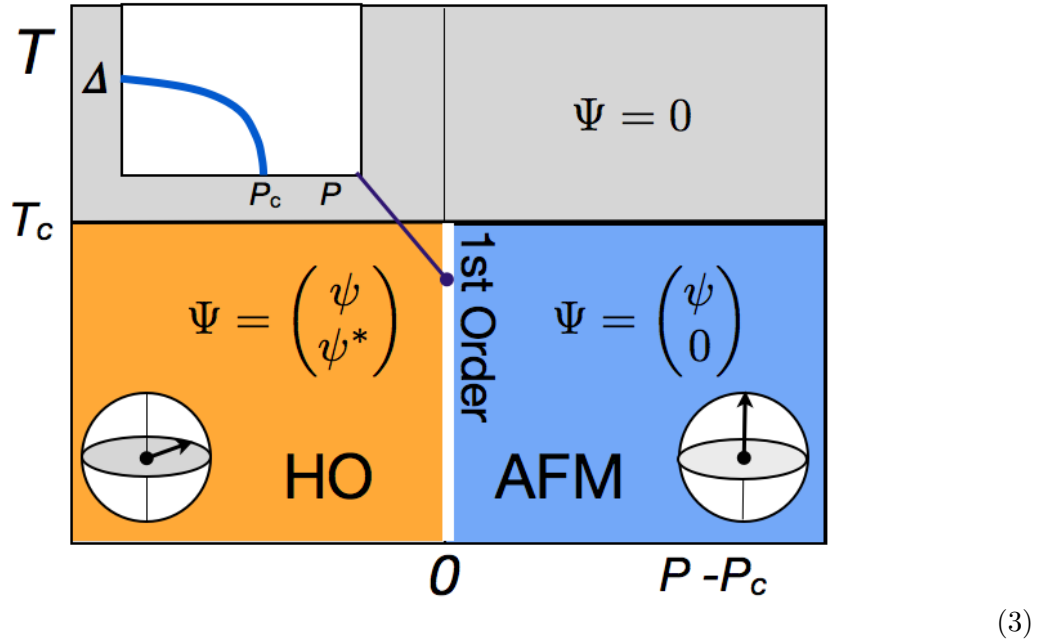


FIG. 1. Global phase diagram predicted by Landau theory.

terms in  $f[\Psi]$ . The variation in the action is then given by

$$\delta S = \rho |\Psi_0|^2 \sum_q |\theta(q)|^2 \left( \vec{q}^2 - \frac{\omega^2}{c^2} + \frac{2\delta}{\rho} (P_c - P) |\Psi_0|^2 \right) \quad (8)$$

The dispersion is therefore

$$\omega^2 = (cq)^2 + \Delta^2 \quad (9)$$

where

$$\Delta^2 = \frac{2\delta(P_c - P)}{\rho} |\Psi_0|^2, \quad (10)$$

so that even though the phase transition at  $P = P_c$  is first order, the gap for longitudinal spin fluctuations is

$$\Delta \propto |\Psi_0| \sqrt{P_c - P}.$$

Since  $dP_c/dT_c$  is finite, close to the transition,  $\sqrt{P_c - P} \approx \sqrt{dP_c/dT_c(T - T_c)}$ , and  $\Delta \propto \sqrt{T - T_c}$ . Inelastic neutron scattering experiments can measure this gap as a function of temperature at a fixed pressure where there is a finite temperature first order transition. The iron-doped compound,  $\text{URu}_{2-x}\text{Fe}_x\text{Si}_2$  can provide an attractive alternative to hydrostatic pressure, as iron doping acts as uniform chemical pressure and tunes the hidden order state into the antiferromagnet[18].

## B. Landau Theory in Magnetic Field: Nonlinear Susceptibility

The origin of the large c-axis nonlinear susceptibility anomaly in  $\text{URu}_2\text{Si}_2$  [10] has been a long-standing mystery. It has been understood phenomenologically within a Landau theory as a consequence of a large  $\Psi^2 B_z^2$  coupling of unknown origin[10, 11]. Here we show that the Landau theory of hastatic order will contain just such a term.

While the conduction electrons couple isotropically to an applied field, the non-Kramers doublet linearly couples only to the z-component of the magnetic field,  $B_z = B \cos \theta$ , which splits the doublet as it begins to suppress the Kondo effect. When we include the effect of the magnetic field in the Landau theory, we obtain:

$$f[\Psi] = [\alpha(T_c - T) - \eta_z B_z^2 - \eta_\perp B_\perp^2] \Psi^2 + \beta |\Psi|^4 + \gamma (\Psi^\dagger \sigma_z \Psi)^2, \quad (11)$$

where we shall show below that the coefficient of the  $\Psi^2 B_z^2$  term,  $\eta_z$  goes as  $\rho/T_{HO}^2$ , where  $\rho$  is the conduction electron density of states, while the coefficient of the  $\Psi^2 B_\perp^2$  term,  $\eta_\perp$  is







#### IV. TWO CHANNEL ANDERSON LATTICE MODEL FOR URU<sub>2</sub>SI<sub>2</sub>

Our model describes a lattice of  $U$  ions immersed in a conduction sea of electrons. We take the low energy configuration of each  $U$  ion to be a  $5f^2$   $\Gamma_5$  non-Kramers doublet. All energies are measured relative to the energy of the isolated doublet. For simplicity, in our model we take the dominant valence fluctuation channel to be  $5f^2 \rightleftharpoons 5f^1$ . Particle-hole symmetry can be used to formulate the equivalent model with fluctuations into a  $5f^3$  Kramers doublet. The full model is then written

$$H = \sum_{\mathbf{k}\sigma} \epsilon_{\mathbf{k}} c_{\mathbf{k}\sigma}^\dagger c_{\mathbf{k}\sigma} + \sum_j (H_{VF}(j) + H_a(j)) \quad (23)$$

where  $c_{\mathbf{k}\sigma}^\dagger$  creates a conduction electron of momentum  $\mathbf{k}$  spin  $\sigma$ , with energy  $\epsilon_{\mathbf{k}}$ ,

$$H_{VF}(j) = V_6 \psi_{\Gamma_6\pm}^\dagger(j) |\Gamma_7^\pm \pm\rangle \langle \Gamma_5 \pm | + V_7 \psi_{\Gamma_7\mp}^\dagger(j) |\Gamma_7^\mp \mp\rangle \langle \Gamma_5 \pm | + \text{H.c.} \quad (24)$$

describes the valence fluctuations between the  $\Gamma_5$  doublet and an excited  $\Gamma_7$  Kramers doublet while

$$H_a(j) = \Delta E \sum_{\pm} |\Gamma_7\pm\rangle \langle \Gamma_7 \pm | \quad (25)$$

is the atomic Hamiltonian.

In our model, we choose the  $\Gamma_7$  to be the lowest excited state; in this case the the valence fluctuations are determined by the decomposition,

$$|\Gamma_7\pm\rangle = \alpha \psi_{\Gamma_6\mp}^\dagger |\Gamma_5\pm\rangle + \beta \psi_{\Gamma_7\mp}^\dagger |\Gamma_5\mp\rangle, \quad (26)$$

where  $\psi_{\Gamma\alpha}^\dagger = \sum_{\mathbf{k}} c_{\mathbf{k}\beta}^\dagger [\Phi_{\Gamma\mathbf{k}}]_{\alpha\beta} e^{-i\mathbf{k}\cdot\mathbf{R}_j}$  creates a conduction electron in a Wannier state with  $j = 5/2$  and symmetry  $\Gamma$  ( $= \Gamma_6, \Gamma_7$ ) localized around the uranium atom at site  $j$ .

For a plane wave, the form factors are given by  $[\Phi_{\Gamma\mathbf{k}}]_{\alpha\beta} = y_{\alpha\beta}^\Gamma(\mathbf{k})$ , where

$$y_{\alpha\beta}^\Gamma(\mathbf{k}) = Y_{3m-\frac{\alpha}{2}}(\hat{\mathbf{k}}) \langle 3m - \frac{\alpha}{2}, \frac{1}{2} \frac{\alpha}{2} | 5/2m \rangle \overbrace{\langle m | \beta \rangle}^{a_m}$$

In URu<sub>2</sub>Si<sub>2</sub>, the uranium atoms are located on a body centered tetragonal lattice (bct) at relative locations,  $\mathbf{R}_{NN} = (\pm a/2, \pm a/2, \pm c/2)$ , while the f-electrons hybridize with conduction electrons located around the silicon atoms,  $\mathbf{a}_{NN} = (\pm a/2, \pm a/2, \pm z)$  where  $z = .371c$  is the height of the silicon atom above the  $U$  atom[3]. The form-factor is then,

$$[\Phi_{\Gamma\mathbf{k}}]_{\alpha\beta} = \sum_{\{\mathbf{R}_{NN}, \mathbf{a}_{NN}\}} e^{-i\mathbf{k}\cdot\mathbf{R}_{NN}} y_{\alpha\beta}^\Gamma(\mathbf{a}_{NN}) \quad (27)$$

Notice that this function has the following properties:  $[\Phi_{\Gamma\mathbf{k}+\mathbf{G}}]_{\alpha\beta} = [\Phi_{\Gamma\mathbf{k}}]_{\alpha\beta}$  and  $[\Phi_{\Gamma\mathbf{k}+\mathbf{Q}}]_{\alpha\beta} = -[\Phi_{\Gamma\mathbf{k}}]_{\alpha\beta}$ .

To cast the Hamiltonian as a field theory, we introduce a slave boson/slave fermion representation,  $|\Gamma_7\sigma\rangle\langle\Gamma_5\alpha| = b_\sigma^\dagger\chi_\alpha$ , where  $b_\sigma^\dagger|\Omega\rangle$  represents the occupation of  $5f^1$ , and  $b_\sigma$  carries a positive charge and  $\chi_\alpha^\dagger|\Omega\rangle$  represents the  $5f^2$  state. The valence fluctuation term in the Hamiltonian then takes the form

$$H_{VF1}(j) = \sum_{\mathbf{k}} c_{\mathbf{k}\sigma}^\dagger \hat{\mathcal{V}}_{\sigma\alpha}^{(1)}(\mathbf{k}, j) \chi_\alpha(j) e^{-i\mathbf{k}\cdot\mathbf{R}_j} + \text{H.c.} \quad (28)$$

Introducing  $\hat{B}^\dagger = \begin{pmatrix} \hat{\Psi}_\uparrow^\dagger & 0 \\ 0 & \hat{\Psi}_\downarrow^\dagger \end{pmatrix}$  (where we use  $\hat{\Psi}_\sigma^\dagger$  instead of the traditional  $b_\sigma^\dagger$  to reinforce that these are indeed order parameters), we can write the hybridization compactly,

$$\hat{\mathcal{V}}^{(1)}(\mathbf{k}, j) = V_6\Phi_{\Gamma_6}B_j^\dagger + V_7\Phi_{\Gamma_7^-}\hat{B}_j^\dagger\sigma_1. \quad (29)$$

In the mean field theory, we replace  $\hat{\mathcal{V}}(\mathbf{k}, j) \rightarrow \langle\hat{\mathcal{V}}(\mathbf{k}, j)\rangle$ , replacing  $\langle\hat{\Psi}_\sigma^\dagger\rangle = \Psi_\sigma^*$ . We consider the configuration

$$\langle\hat{B}_j^\dagger\rangle = |\Psi| \begin{pmatrix} e^{i(\mathbf{Q}\cdot\mathbf{R}_j+\phi)/2} & \\ & e^{-i(\mathbf{Q}\cdot\mathbf{R}_j+\phi)/2} \end{pmatrix} = |\Psi|U_j \quad (30)$$

where  $U_j$  is a unitary matrix. and  $\mathbf{Q} = (0, 0, \frac{2\pi}{c})$  is the common wavevector for hastatic order, chosen to match the antiferromagnet, and  $\phi = \pi/4$  is chosen to match the susceptibility anisotropy. It is convenient to redefine  $\tilde{\chi}_j = U_j\chi_j$ . With this device, the spatial dependence of  $\langle\hat{B}_j^\dagger\rangle$  is absorbed into the redefined f-electrons, so that  $\hat{B}_j^\dagger\chi_j = |\Psi|\tilde{\chi}_j$  and

$$\hat{B}_j^\dagger\sigma_1\chi_j = |\Psi|(U_j\sigma_1U_j^\dagger)\tilde{\chi}_j = |\Psi|(\hat{\mathbf{n}}\cdot\vec{\sigma})e^{i\mathbf{Q}\cdot\mathbf{R}_j}\tilde{\chi}_j, \quad \hat{\mathbf{n}} = \frac{1}{\sqrt{2}}(\hat{\mathbf{x}} + \hat{\mathbf{y}}). \quad (31)$$

In this gauge, the  $\Gamma_6$  hybridization is uniform while the  $\Gamma_7^-$  hybridization is staggered. We write  $\mathcal{V}_6(\mathbf{k}) = |\Psi|V_6\Phi_{\Gamma_6}$ , and  $\mathcal{V}_7(\mathbf{k}) = |\Psi|V_7\Phi_{\Gamma_7}(\hat{\mathbf{n}}\cdot\vec{\sigma})$ .

In the slave formulation, the atomic Hamiltonian is  $H_a(j) = \Delta E \sum_\sigma \Psi_{j\sigma}^\dagger \Psi_{j\sigma}$ . The introduction of slave bosons and fermions to represent the Hubbard operators requires a constraint to maintain one particle per site,  $\lambda_j \left( \sum_\sigma \Psi_{j\sigma}^\dagger \Psi_{j\sigma} + \sum_\alpha \chi_{j\alpha}^\dagger \chi_{j\alpha} - 1 \right)$ .

We take a simplified model of the conduction electron hopping, treating them as s-wave electrons located at the  $U$  site, hopping on a bct lattice with dispersion

$$\epsilon_{\mathbf{k}} = -8t \cos \frac{k_x a}{2} \cos \frac{k_y a}{2} \cos \frac{k_z c}{2} - \mu. \quad (32)$$

We do, however, want to capture the essential characteristics of the URu<sub>2</sub>Si<sub>2</sub> bandstructure - namely nesting between an electron Fermi surface about the zone center and a hole Fermi surface at  $\mathbf{Q}$ [3]. In order to favor a staggered hybridization, and to match up with ARPES experiments suggesting a heavy f-band[2], we take the hole Fermi surface to be generated from a weakly dispersion  $\chi$  band. This f-electron hopping will be naturally generated by hybridization fluctuations above  $T_{HO}$ , effectively where  $\langle \hat{B}^\dagger \hat{B} \rangle \neq 0$  while  $\langle \hat{B} \rangle = 0$ . A large  $N$  expansion of this problem would capture these fluctuation effects, but is overly complicated for this problem so we put this dispersion in by hand,  $\epsilon_{f\mathbf{k}} = -8t_f \cos \frac{k_x a}{2} \cos \frac{k_y a}{2} \cos \frac{k_z c}{2}$ .

So to summarize, our mean-field Hamiltonian is,

$$H = \sum_{\mathbf{k}} \epsilon_{\mathbf{k}} c_{\mathbf{k}\sigma}^\dagger c_{\mathbf{k}\sigma} + \sum_{\mathbf{k}} t f_{\mathbf{k}} \chi_{\mathbf{k}\eta}^\dagger \chi_{\mathbf{k}\eta} + \sum_j (\Delta E + \lambda_j) \Psi_{j\sigma}^\dagger \Psi_{j\sigma} + \lambda_j (\chi_{j\eta}^\dagger \chi_{j\eta} - 1) + \sum_j H_{VF}(j). \quad (33)$$

We rewrite this Hamiltonian in matrix form

$$H = \sum_{\mathbf{k}} \left( c_{\mathbf{k}}^\dagger, c_{\mathbf{k}+\mathbf{Q}}^\dagger, \chi_{\mathbf{k}}^\dagger, \chi_{\mathbf{k}+\mathbf{Q}}^\dagger \right) \overbrace{\begin{pmatrix} \epsilon_{\mathbf{k}} & 0 & \mathcal{V}_6(\mathbf{k}) & \mathcal{V}_7(\mathbf{k}) \\ 0 & \epsilon_{\mathbf{k}+\mathbf{Q}} & -\mathcal{V}_7(\mathbf{k}) & -\mathcal{V}_6(\mathbf{k}) \\ \mathcal{V}_6^\dagger(\mathbf{k}) & -\mathcal{V}_7^\dagger(\mathbf{k}) & \lambda_{\mathbf{k}} & 0 \\ \mathcal{V}_7^\dagger(\mathbf{k}) & -\mathcal{V}_6^\dagger(\mathbf{k}) & 0 & \lambda_{\mathbf{k}+\mathbf{Q}} \end{pmatrix}}^{\mathcal{H}_{\alpha\beta}(\mathbf{k})} \begin{pmatrix} c_{\mathbf{k}} \\ c_{\mathbf{k}+\mathbf{Q}} \\ \chi_{\mathbf{k}} \\ \chi_{\mathbf{k}+\mathbf{Q}} \end{pmatrix} + \sum_j \left[ (\Delta E + \lambda) \Psi_{j\sigma}^\dagger \Psi_{j\sigma} - \lambda \right]. \quad (34)$$

where we have suppressed spin indices, made the assumption that  $\lambda_j = \lambda$  is uniform, equivalent to enforcing the constraint on average, introduced  $\lambda_{\mathbf{k}} = \lambda - \epsilon_{f\mathbf{k}}$ , and used the simplification that  $\mathbf{Q}$  is half a reciprocal lattice vector, making  $\mathcal{V}(\mathbf{k} + \mathbf{Q}) = -\mathcal{V}(\mathbf{k})$ , as shown above.

In the absence of particle-hole symmetry, this Hamiltonian cannot be diagonalized analytically, and must be done numerically, giving a set of four doubly degenerate bands,  $E_{\mathbf{k}\eta}$ . The mean field free energy is,

$$F[b, \lambda] = -\frac{\beta^{-1}}{2} \sum_{\mathbf{k}, \eta} \log [1 + e^{-\beta E_{\mathbf{k}\eta}}] + \mathcal{N}_s [2(\Delta E + \lambda)|\Psi|^2 - \lambda], \quad (35)$$

where  $\beta = (k_B T)^{-1}$ . The mean field parameters,  $|\Psi|$  and  $\lambda$  are obtained by numerically finding a stationary point of the free energy that minimizes  $F$  with respect to  $|\Psi|$  and maximizes it with respect to  $\lambda$ . A plot of  $|\Psi|$  and  $\lambda$  as a function of temperature is shown

in Figure 1 C, for the parameters used to calculate  $\chi_{xy}(T)$  and  $m(T)$  for Figure in the main paper. The parameters are as follows:  $t = 12.5$  meV is taken to match the magnitude of  $\chi_{xy}$  from the torque magnetometry data[6].  $\mu/t = -.075$  gives the slight particle-hole asymmetry essential to reproduce the flattening of  $\chi_{xy}$  at low temperatures, and has also been adjusted so that  $\mu + \lambda = 0$  at  $T = 0$  for consistency with the dI/dV calculations;  $t_f/t = -.025$  gives a weak f-electron dispersion; the crystal field angle  $\xi = .05$  is taken to be small, as it is in CeRu<sub>2</sub>Si<sub>2</sub>[4];  $V_6/V_7 = 1$  is arbitrary; and finally  $V^2/\Delta E = 2t$  is chosen to give  $2|\Psi|^2 \approx 15\%$  mixed valency. The shape of the susceptibility curve is quite sensitive to the particle-hole asymmetry and degree of mixed valency, but not to the other parameters. The internal angle,  $\phi$  controls the susceptibility anisotropy and the orientation of the magnetic moments.  $\phi = \pi/4$  reproduces  $\chi_{xy} \neq 0$ ,  $\chi_{xx} = \chi_{yy}$ .

It is important to note that the hastatic state is promoted by a partial nesting of the normal state Fermi surface along  $\mathbf{Q} = (100)$ , leading to the partial gapping of the Fermi

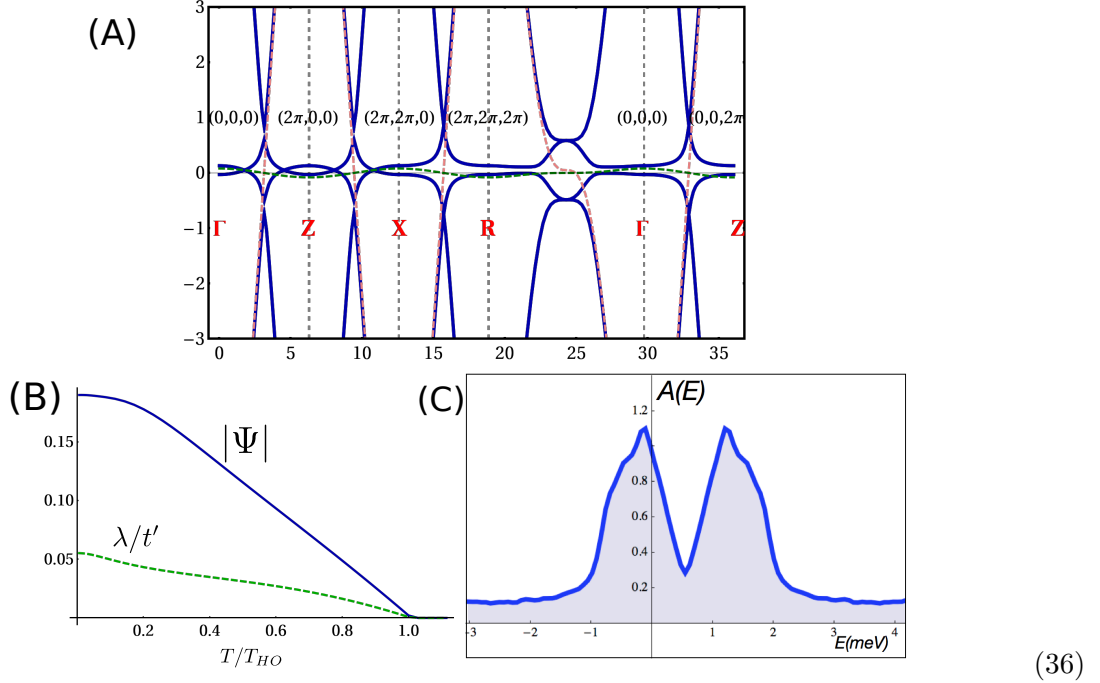


FIG. 2. (A) Band structure of the hastatic order is shown in solid blue, while the bare conduction (red) and f (green) bands are dashed. (B) Mean field parameters  $|\Psi|$  and  $\lambda$  as a function of temperature. (C) Density of states in hastatic order, for the region close to the Fermi energy containing the hybridization gap.

surface seen in the density of states (Fig. 2C). However, even for perfect nesting, there will still be gapless excitations, as the hybridization gap,  $\mathcal{V}_6^\dagger \mathcal{V}_7$  contains a node along the c-axis (due to a c-axis node in  $\mathcal{V}_7$ ). In this sense (and this sense only), the hastatic state is similar to the Ikeda-Miyake model[16] of the failed Kondo insulators CeNiSn and CeRhSb, which also predicts a gapless state.

Above  $T_{HO}$  in URu<sub>2</sub>Si<sub>2</sub>, there are magnetic fluctuations seen at two momentum transfers: at the commensurate  $\mathbf{Q} = (1, 0, 0)$ , which goes soft at  $T_{HO}$  and at the incommensurate  $\mathbf{Q}^* = (1 \pm .4, 0, 0)$ , which remains at finite energy above both the HO and AFM phases[12]. While we have chosen a simplified bandstructure that captures the partial nesting at the commensurate  $\mathbf{Q}$ , it is likely that a more realistic bandstructure will contain other energetically competitive nesting vectors that never develop due to the stronger nesting at  $\mathbf{Q}$ . Fluctuations induced by these nearby phases could be captured within an RPA treatment of a model with a more realistic bandstructure.

For simplicity we have discussed the two channel Anderson model involving fluctuations from a  $5f^2$   $\Gamma_5$  ground state to  $5f^1$  ( $J = 5/2$ ). However, the more realistic case involves fluctuations to  $5f^3$ , whose low energy states have  $J = 9/2$ , and are split into five Kramers doublets by the tetragonal crystal field,

$$\begin{aligned} |\Gamma_7^1 \pm\rangle &= a|\pm 5/2\rangle + b|\mp 3/2\rangle \\ |\Gamma_7^2 \pm\rangle &= -b|\pm 5/2\rangle + a|\mp 3/2\rangle \\ |\Gamma_6^{1,2,3} \pm\rangle &= c^{1,2,3}|\pm 9/2\rangle + d^{1,2,3}|\pm 1/2\rangle + e^{1,2,3}|\mp 7/2\rangle. \end{aligned} \quad (37)$$

There are two generic situations: either a  $\Gamma_7$  doublet will be lowest in energy, and the valence fluctuations will be determined by the overlap,

$$|\Gamma_7 \pm\rangle = \alpha \psi_{6\mp}^\dagger |\Gamma_5 \pm\rangle + \beta \psi_{7\mp}^\dagger |\Gamma_5 \mp\rangle, \quad (38)$$

or a  $\Gamma_6$  doublet will be lowest in energy, with the relevant overlap,

$$|\Gamma_6 \pm\rangle = \alpha \psi_{7\mp}^\dagger |\Gamma_5 \pm\rangle + \beta \psi_{6\mp}^\dagger |\Gamma_5 \mp\rangle, \quad (39)$$

where the form-factors are as above. In both cases fluctuations will involve conduction electrons in both  $\Gamma_6$  and  $\Gamma_7$  symmetries. When the lowest excited state is a  $\Gamma_7$ , the valence fluctuation Hamiltonian is given by,

$$H_{VF3}(j) = V_6 \psi_{j\Gamma_6\mp}^\dagger |\Gamma_5 \pm\rangle \langle \Gamma_7 \pm | + V_7 \psi_{j\Gamma_7\mp}^\dagger |\Gamma_5 \mp\rangle \langle \Gamma_7 \pm | + \text{H.c.} \quad (40)$$

Now we can follow the same slave boson procedure as discussed previous, where  $\Psi_\sigma^\dagger$  now represents a  $5f^3$  state and carries a negative charge, and the valence fluctuation term is the particle-hole conjugate of the  $5f^1$  case,  $c_{\mathbf{k}\sigma}^\dagger \hat{\mathcal{V}}_{\sigma\alpha}(\mathbf{k}, j) \chi_\alpha^*(j) e^{-i\mathbf{k} \cdot \mathbf{R}_j}$ . If we perform a particle-hole transformation on  $\chi$ , we regain the Hamiltonian, (34) with only a sign change for  $\lambda_{\mathbf{k}}$ .

## V. MAGNETIZATION AND SUSCEPTIBILITY CALCULATION

The uniform basal plane conduction electron magnetic susceptibility is

$$\chi^{xy} = -(g\mu_B)^2 T \sum_{i\omega_n} \sum_{\mathbf{k}} \text{Tr} [\sigma^x \mathcal{G}^c(\mathbf{k}, \mathbf{k} + \mathbf{Q}, i\omega_n) \sigma^y \mathcal{G}^c(\mathbf{k} + \mathbf{Q}, \mathbf{k}, i\omega_n)], \quad (41)$$

while the staggered conduction electron magnetization is

$$\vec{m}_c(\mathbf{Q}) = -g\mu_B T \sum_{i\omega_n} \sum_{\mathbf{k}} \text{Tr} \vec{\sigma} \mathcal{G}^c(\mathbf{k}, \mathbf{k} + \mathbf{Q}, i\omega_n) \quad (42)$$

In order to calculate these, we require the full conduction electron Green's function, which can be found from the Hamiltonian by integrating out the f-electrons,

$$[\mathcal{G}^c(\mathbf{k}, i\omega)]^{-1} = \begin{pmatrix} i\omega_n - \epsilon_{\mathbf{k}} & 0 \\ 0 & i\omega_n - \epsilon_{\mathbf{k}+\mathbf{Q}} \end{pmatrix} - \mathcal{V}_{\mathbf{k}} \begin{pmatrix} i\omega_n - \lambda_{\mathbf{k}} & 0 \\ 0 & i\omega_n - \lambda_{\mathbf{k}+\mathbf{Q}} \end{pmatrix}^{-1} \mathcal{V}_{\mathbf{k}}^\dagger, \quad (43)$$

where

$$\mathcal{V}_{\mathbf{k}} = \begin{pmatrix} \mathcal{V}_{6\mathbf{k}} & \mathcal{V}_{7\mathbf{k}} \\ -\mathcal{V}_{7\mathbf{k}} & -\mathcal{V}_{6\mathbf{k}} \end{pmatrix}. \quad (44)$$

Using isospin,  $\vec{\tau}$  to represent  $\mathbf{k}, \mathbf{k}+\mathbf{Q}$  space, we split the conduction electron energy,  $\epsilon_{\mathbf{k}}$  into  $\epsilon_{0\mathbf{k}} = \frac{1}{2}(\epsilon_{\mathbf{k}} + \epsilon_{\mathbf{k}+\mathbf{Q}})$ ,  $\epsilon_{1\mathbf{k}} = \frac{1}{2}(\epsilon_{\mathbf{k}} - \epsilon_{\mathbf{k}+\mathbf{Q}})$  into the particle-hole symmetric and antisymmetric parts (and similarly with  $\lambda_{0\mathbf{k}}, \lambda_{1\mathbf{k}}$ ). So now we can write the conduction electron Green's function as:

$$[\mathcal{G}^c(\mathbf{k}, i\omega)]^{-1} = (i\omega_n - \epsilon_{0\mathbf{k}}) - \epsilon_{1\mathbf{k}}\tau_3 - \mathcal{V} \frac{i\omega_n - \lambda_{0\mathbf{k}} + \lambda_{1\mathbf{k}}\tau_3}{(i\omega_n - \lambda_{0\mathbf{k}})^2 - \lambda_{1\mathbf{k}}^2} \mathcal{V}^\dagger \quad (45)$$

For completeness, the f-electron Green's function will be,

$$[\mathcal{G}^f(\mathbf{k}, i\omega)]^{-1} = (i\omega_n - \lambda_{0\mathbf{k}}) - \lambda_{1\mathbf{k}}\tau_3 - \mathcal{V}^\dagger \frac{i\omega_n - \epsilon_{0\mathbf{k}} + \epsilon_{1\mathbf{k}}\tau_3}{(i\omega_n - \epsilon_{0\mathbf{k}})^2 - \epsilon_{1\mathbf{k}}^2} \mathcal{V}. \quad (46)$$



The Green's function can be expanded in terms of  $\vec{\tau} \otimes \vec{\sigma}$ , where  $\vec{\sigma}$  describes the spin. To do so, we take  $\text{Tr} \mathcal{V} \mathcal{V}^\dagger \tau_a \sigma_b$  and  $\text{Tr} \mathcal{V} \tau_3 \mathcal{V}^\dagger \tau_a \sigma_b$ . The relevant parameters are:

$$\begin{aligned}
V_{\mathbf{k}+}^2 &= \text{Tr} \mathcal{V}_{\mathbf{k}} \mathcal{V}_{\mathbf{k}}^\dagger = 2\text{Tr} \left[ \mathcal{V}_{6\mathbf{k}} \mathcal{V}_{6\mathbf{k}}^\dagger + \mathcal{V}_{7\mathbf{k}} \mathcal{V}_{7\mathbf{k}}^\dagger \right] \\
V_{\mathbf{k}-}^2 &= \text{Tr} \mathcal{V}_{\mathbf{k}} \tau_3 \mathcal{V}_{\mathbf{k}}^\dagger \tau_3 = 2\text{Tr} \left[ \mathcal{V}_{6\mathbf{k}} \mathcal{V}_{6\mathbf{k}}^\dagger - \mathcal{V}_{7\mathbf{k}} \mathcal{V}_{7\mathbf{k}}^\dagger \right] \\
\Delta_{\mathbf{k}-} &= \text{Tr} \mathcal{V}_{\mathbf{k}} \tau_3 \mathcal{V}_{\mathbf{k}}^\dagger \tau_2 = 2i\text{Tr} \left[ \mathcal{V}_{6\mathbf{k}} \mathcal{V}_{7\mathbf{k}}^\dagger - \mathcal{V}_{7\mathbf{k}} \mathcal{V}_{6\mathbf{k}}^\dagger \right] \\
\vec{\Delta}_{\mathbf{k}+} &= \text{Tr} \mathcal{V}_{\mathbf{k}} \mathcal{V}_{\mathbf{k}}^\dagger \tau_1 \vec{\sigma} = 2\text{Tr} \left[ \left( \mathcal{V}_{6\mathbf{k}} \mathcal{V}_{7\mathbf{k}}^\dagger + \mathcal{V}_{7\mathbf{k}} \mathcal{V}_{6\mathbf{k}}^\dagger \right) \vec{\sigma} \right].
\end{aligned} \tag{47}$$

All other combinations are uniformly zero. The conduction electron Green's function can be written in the form  $[\mathcal{G}^c]^{-1} = A\tau_0 + B\tau_3 + \vec{C} \cdot \vec{\sigma}\tau_1 + D\tau_2$ . The eigenvalues are found by taking  $\det [\mathcal{G}^c(\mathbf{k}, \omega)]^{-1} = 0$ , leading to an eighth order polynomial. For the special particle-hole symmetric case where  $\epsilon_0 = \lambda_0 = 0$ , this reduces to  $\omega^4 - 2\alpha_{\mathbf{k}}\omega^2 - \gamma_{\mathbf{k}}^2$ , which can be solved analytically. The four (doubly degenerate) eigenvalues are  $E_{\mathbf{k}\eta}$  and are found numerically on a grid of  $\mathbf{k}$  points. Due to the structure of the Green's function, we can write,

$$\begin{aligned}
\mathcal{G}^c(i\omega_n, \mathbf{k}) &= \frac{1}{\prod_{\eta} (i\omega_n - E_{\mathbf{k}\eta})} \left( A\tau_0 - B\tau_3 - \vec{C} \cdot \vec{\sigma}\tau_1 - D\tau_2 \right), \\
A &= (i\omega_n - \epsilon_{0\mathbf{k}}) \left[ (i\omega_n - \lambda_{0\mathbf{k}})^2 - \lambda_{1\mathbf{k}}^2 \right] - (i\omega_n - \lambda_{0\mathbf{k}}) V_{\mathbf{k}+}^2 \\
B &= -\epsilon_{1\mathbf{k}} \left[ (i\omega_n - \lambda_{0\mathbf{k}})^2 - \lambda_{1\mathbf{k}}^2 \right] - \lambda_{1\mathbf{k}} V_{\mathbf{k}-}^2 \\
\vec{C} &= -(i\omega_n - \lambda_{0\mathbf{k}}) \vec{\Delta}_{\mathbf{k}+} \\
D &= -\lambda_{1\mathbf{k}} \Delta_{\mathbf{k}-}
\end{aligned} \tag{48}$$

which makes it particularly easy to write down the conduction electron magnetization,

$$\begin{aligned}
\vec{m}_c(\mathbf{Q}) &= -(g\mu_B)T \sum_{\mathbf{k}, \omega_n} \text{Tr} [\vec{\sigma} \mathcal{G}^c(\mathbf{k}, i\omega_n) \tau_1] \\
&= -(g\mu_B) \sum_{\mathbf{k}\eta} \frac{(E_{\mathbf{k}\eta} - \lambda_{0\mathbf{k}})}{\prod_{\eta' \neq \eta} (E_{\mathbf{k}\eta} - E_{\mathbf{k}\eta'})} f(E_{\mathbf{k}\eta}) \vec{\Delta}_{\mathbf{k}+}
\end{aligned} \tag{49}$$

and susceptibility,

$$\begin{aligned}
\chi^{xy} &= -(g\mu_B)^2 T \sum_{i\omega_n} \sum_{\mathbf{k}} \text{Tr} [\sigma_x \mathcal{G}^c(\mathbf{k}, i\omega_n) \sigma_y \mathcal{G}^c(\mathbf{k}, i\omega_n)] \\
&= -(g\mu_B)^2 \sum_{\mathbf{k}\eta} \left[ \frac{2(E_{\mathbf{k}\eta} - \lambda_{0\mathbf{k}}) f(E_{\mathbf{k}\eta}) + (E_{\mathbf{k}\eta} - \lambda_{0\mathbf{k}})^2 f'(E_{\mathbf{k}\eta})}{\prod_{\eta' \neq \eta} (E_{\mathbf{k}\eta} - E_{\mathbf{k}\eta'})^2} \right. \\
&\quad \left. - \sum_{\eta' \neq \eta} \frac{2(E_{\mathbf{k}\eta} - \lambda_{0\mathbf{k}})^2 f(E_{\mathbf{k}\eta})}{(E_{\mathbf{k}\eta} - E_{\mathbf{k}\eta'}) \prod_{\eta'' \neq \eta} (E_{\mathbf{k}\eta} - E_{\mathbf{k}\eta''})^2} \right] \Delta_{\mathbf{k}+}^x \Delta_{\mathbf{k}+}^y
\end{aligned} \tag{50}$$

Note that above integral may be positive or negative. The functions  $f$  and  $f'$  are the Fermi function,  $f(x) = (e^{-x/T} + 1)^{-1}$  and it's derivative,  $f'(x) = df(x)/dx$ , respectively.

Although the conduction electrons develop a magnetic moment, the f-electrons have no dipolar or quadrupolar moments,  $\vec{m}_f = 0$ . Upon closer examination, the quadrupolar moments are found to vanish because of a d-wave form factor, implying that there is no net quadrupole moment and thus no associated lattice distortion, even for uniform hastatic order. As a d-wave quadrupole is a hexadecapole, this ultimately means that like Haule and Kotliar[5], we have staggered  $(J_x J_y + J_y J_x)(J_x^2 - J_y^2)$  hexadecapolar moments. However, unlike Haule and Kotliar, where the hexadecapolar moments are the primary order parameter (and thus of order one), here the hexadecapolar moments are a secondary effect of the composite hastatic order, and like the conduction electron moments, will be of order  $T_K/D$ . The f-electron moment has an identical form to the conduction electron moment, (37), with  $\epsilon \leftrightarrow \lambda$  everywhere, and the relevant form-factor becomes  $\vec{\Delta}_{\mathbf{k}+}^f = \text{Tr} \mathcal{V}_{\mathbf{k}} \vec{\sigma} \tau_1 \mathcal{V}_{\mathbf{k}}^\dagger$ . Given how difficult it is to observe large hexadecapolar moments, the hexadecapolar moments associated with hastatic order will almost certainly be unobservably small. By contrast, in the antiferromagnetic phase, the f-electrons develop a large c-axis magnetic moment.

## VI. CURRENT NEUTRON SCATTERING BOUNDS ON THE TRANSVERSE MOMENT

We predict a staggered basal plane magnetic moment on the order of  $.01\mu_B/U$ . However, such a moment has not been previously detected, despite a large number of neutron studies. Early neutron studies focused on the small,  $.02 - .04\mu_B$  c-axis moment[13, 14], which was later shown to be due to small, local regions of large moment antiferromagnetism[15]. Such inhomogeneous antiferromagnetism persists even in high quality single crystals, making it essential to identify the moment orientation. The moment orientation has not been examined since these early works[13, 14], whose resolution of  $.01\mu_B$  is on the order of our prediction. As the neutron signal is proportional to the component of the moment perpendicular to  $\mathbf{Q}$ :  $\mathbf{m}_\perp \propto \mathbf{Q} \times (\mathbf{m} \times \mathbf{Q})$ , measuring along  $\mathbf{Q} = (001)$  will isolate the transverse magnetic moment. More recent studies have focused on  $\mathbf{Q} = (100)$ , where the extrinsic c-axis moment is always seen[12]. Detection of our predicted  $\mathbf{m}_\perp$  will require high resolution, likely spin-polarized, measurements along  $\mathbf{Q} = (001)$ .

## VII. DENSITY OF STATES

To simplify the calculation of the ground-state properties, we have taken  $\epsilon_{0\mathbf{k}} = -\mu$  and  $\lambda_{0\mathbf{k}} = \lambda$  to be constant, and chosen the filling of the conduction sea so that at  $T = 0$ ,  $\lambda + \mu = 0$ . In this case, the Hamiltonian  $\mathcal{H}(\mathbf{k})_{\alpha\beta}$  in (34) can be diagonalized analytically, leading to four doublets  $|\mathbf{k}\eta\sigma\rangle$  ( $\sigma = \pm 1$ ), with eigenvectors

$$u_\alpha(\mathbf{k}\eta\sigma) = \langle \alpha | \mathbf{k}\eta\sigma \rangle \quad (51)$$

such that  $\mathcal{H}_{\alpha\beta}(\mathbf{k}) \cdot u(\mathbf{k}\eta\sigma) = E_{\mathbf{k}\eta} u(\mathbf{k}\eta\sigma)$ . The degeneracy of the eigenvalues is guaranteed by the invariance of the Hamiltonian under time-reversal plus a translation by  $\mathbf{Q}$ . The energies  $E_{\mathbf{k}\eta}$  are given by

$$E_{\mathbf{k}\eta} = \left\{ \lambda \pm \sqrt{\alpha_{\mathbf{k}} \pm \sqrt{\alpha_{\mathbf{k}}^2 - \gamma_{\mathbf{k}}^2}} \right\} \quad (52)$$

where  $\alpha_{\mathbf{k}} = V_{\mathbf{k}+}^2 + \frac{1}{2}(\epsilon_{1\mathbf{k}}^2 + \lambda_{1\mathbf{k}}^2)$  and  $\gamma_{\mathbf{k}}^2 = (\epsilon_{1\mathbf{k}}\lambda_{1\mathbf{k}} - V_{\mathbf{k}-}^2)^2 + (\vec{\Delta}_{\mathbf{k}-})^2$ .

The total density of states is then given by

$$A(\omega) = \sum_{\mathbf{k}\eta} \delta(\omega - E_{\mathbf{k}\eta}) = \frac{1}{\pi} \text{Im} \int \frac{d^3k}{(2\pi)^3} \sum_{\eta} \frac{1}{\omega - E_{\mathbf{k}\eta} - i\delta} \quad (53)$$

where the integral is over the Brillouin zone. Numerically, this quantity was computed by a sum over a discrete set of momenta, dividing the Brillouin zone into  $40^3$  points and using a small value of  $\delta$  to broaden the delta-function into a Lorentzian.

## VIII. G-FACTORS

The Zeeman energy is determined by the Hamiltonian

$$-\vec{B} \cdot \vec{M} = - \sum_{\mathbf{k} \in \frac{1}{2}BZ} \psi_{\mathbf{k}}^\dagger \vec{M} \psi_{\mathbf{k}} \cdot \vec{B} \quad (54)$$

where  $\psi_{\mathbf{k}} = (c_{\mathbf{k}}, c_{\mathbf{k}+\mathbf{Q}}, \chi_{\mathbf{k}}, \chi_{\mathbf{k}+\mathbf{Q}})^T$  and

$$\vec{M} = \frac{1}{2} \begin{pmatrix} 2\mu_B \vec{\sigma} & 0 & 0 & 0 \\ 0 & 2\mu_B \vec{\sigma} & 0 & 0 \\ 0 & 0 & g_f \mu_B \sigma^z & 0 \\ 0 & 0 & 0 & g_f \mu_B \sigma^z \end{pmatrix}, \quad (55)$$

where  $g_f$  is the effective g-factor of the Ising Kramers doublet. In a field, the doubly-degenerate energies,  $|\mathbf{k}\eta\sigma\rangle$  ( $\sigma = \pm 1$ ) are split apart so that  $\Delta E_{\mathbf{k}\eta} = |E_{\mathbf{k}\eta\uparrow} - E_{\mathbf{k}\eta\downarrow}| = g_{\mathbf{k}\eta}(\theta)B$ , so the g-factor is given by  $g_{\mathbf{k}\eta}(\theta) = \left| \frac{d\Delta E_{\mathbf{k}\eta}}{dB} \right|_{B \rightarrow 0}$ . Now we are interested in the Fermi surface average of the g-factor, given by

$$g(\theta) = \frac{\sum_{\mathbf{k}\eta} g_{\mathbf{k}\eta}(\theta) \delta(E_{\mathbf{k}\eta})}{\sum_{\mathbf{k}\eta} \delta(E_{\mathbf{k}\eta})}$$

These quantities were calculated numerically, on a  $40^3$  grid, using  $g_f = 2.9$  for the effective g-factor of the local Kramers doublet. The resulting g-factor in the  $z$ -direction is reduced to  $g_{eff}(\theta = 0) = 2.6$  because of the admixture with conduction electrons. The delta-functions were treated as narrow Lorentzians  $\delta(E) = \frac{1}{\pi} \text{Im}(E - i\eta)^{-1}$ , where  $\eta$  is a small positive number. The g-factors at each point in momentum space were computed by introducing a small field  $\delta B$  into the Hamiltonian, with the approximation  $g_{\mathbf{k}\eta}(\theta) = |E_{\mathbf{k}\uparrow} - E_{\mathbf{k}\downarrow}|/\delta B$ .

## IX. MODEL TUNNELING CONDUCTANCE AND NEMATICITY CALCULATION

To calculate the tunneling density of states, we assume that the differential conductance is proportional to the local Green's function on the surface of the material

$$\frac{dI}{dV}(\mathbf{x}) \propto A(\mathbf{x}, eV) \quad (56)$$

where

$$A(\mathbf{x}, \omega) = \frac{1}{\pi} \text{Im} G_{\sigma\sigma}(x, \omega - i\delta) = \sum_{\sigma} \int_{-\infty}^{\infty} dt \langle \{ \psi_{\sigma}(\mathbf{x}, t), \psi_{\sigma}^{\dagger}(\mathbf{x}, 0) \} \rangle e^{i\omega t}$$

is the imaginary part of the local electronic Green's function. To calculate this quantity, we decompose the local electron field in terms of the low energy fermion modes of the system, writing

$$\psi_{\sigma}(\mathbf{x}) = \sum_j [\phi_c(|\mathbf{x} - \mathbf{R}_j|) c_{j\sigma} + \phi_{\sigma\alpha}^6(\mathbf{x} - \mathbf{R}_j) f_{j\Gamma_6\alpha} + \phi_{\sigma\alpha}^7(\mathbf{x} - \mathbf{R}_j) f_{j\Gamma_7\alpha}] \quad (57)$$

where  $\phi_c(|\mathbf{x} - \mathbf{R}_j|)$  is the wavefunction of the conduction electron centered at site  $j$ , while

$$\begin{aligned} \phi_{\sigma\alpha}^6 &= \phi^6(|\mathbf{x} - \mathbf{R}_j|) \mathcal{Y}_{\sigma\alpha}^6(\mathbf{x} - \mathbf{R}_j) \\ \phi_{\sigma\alpha}^7 &= \phi^7(|\mathbf{x} - \mathbf{R}_j|) \mathcal{Y}_{\sigma\alpha}^7(\mathbf{x} - \mathbf{R}_j) \end{aligned} \quad (58)$$

are the wave functions of the  $\Gamma_6$  and  $\Gamma_{7-}$  f-orbitals centered at site  $j$ .

Projected into the low energy subspace, we have  $f_{j\Gamma_{6\alpha}} \rightarrow (\langle B_j^\dagger \rangle \chi_j)_\alpha$  and  $f_{j\Gamma_{7\alpha}} \rightarrow (\langle B_j^\dagger \rangle \sigma_1 \chi_j)_\alpha$ . Writing  $B_j^\dagger = bU_j$ , and  $\tilde{\chi}_j = U_j \chi_j$  these expressions become  $f_{j\Gamma_{6\alpha}} \rightarrow b\tilde{\chi}_j$  and  $f_{j\Gamma_{7\alpha}} \rightarrow b(\hat{\mathbf{n}} \cdot \vec{\sigma})e^{-i\mathbf{Q} \cdot \mathbf{R}_j} \tilde{\chi}_j$ . Making these substitutions and rewriting the field operators in momentum space we obtain

$$\psi_\sigma(\mathbf{x}) = \sum_{j\mathbf{k} \in \frac{1}{2}BZ} e^{-i\mathbf{k} \cdot \mathbf{R}_j} \Lambda_j(\mathbf{x} - \mathbf{R}_j) \cdot \begin{pmatrix} c_{\mathbf{k}\alpha} \\ c_{\mathbf{k}+\mathbf{Q}\alpha} \\ \chi_{\mathbf{k}\alpha} \\ \chi_{\mathbf{k}+\mathbf{Q}\alpha} \end{pmatrix} \quad (59)$$

where

$$\Lambda_j(\mathbf{x}) = (\phi_c(|\mathbf{x}|)\delta_{\sigma\alpha}, e^{-i\mathbf{Q} \cdot \mathbf{R}_j} \phi_c(|\mathbf{x}|)\delta_{\sigma\alpha}, b\phi_{\sigma\alpha}^6(\mathbf{x}) + e^{-i\mathbf{Q} \cdot \mathbf{R}_j} b\phi_{\sigma\alpha}^7(\mathbf{x})(\hat{\mathbf{n}} \cdot \vec{\sigma}), e^{-i\mathbf{Q} \cdot \mathbf{R}_j} b\phi_{\sigma\alpha}^6(\mathbf{x}) + b\phi_{\sigma\alpha}^7(\mathbf{x})(\hat{\mathbf{n}} \cdot \vec{\sigma})) \quad (60)$$

We choose a layer where  $e^{-i(\mathbf{Q} \cdot \mathbf{R}_j)} = +1$ , then on this layer the local Green's function is given by

$$G(\mathbf{x}, \omega) = \sum_{j,l} \tilde{\Lambda}(\mathbf{x} - \mathbf{R}_j) \cdot \mathcal{G}_{jl}(\omega) \cdot \tilde{\Lambda}^\dagger(\mathbf{x} - \mathbf{R}_l) \quad (61)$$

where

$$\mathcal{G}_{jl}(\omega) = \sum_{\mathbf{k} \in \frac{1}{2}BZ} \text{Tr}[(1 + \tau_1)\mathcal{G}(\mathbf{k}, \omega)] e^{-i\mathbf{k} \cdot (\mathbf{R}_j - \mathbf{R}_l)}$$

is a trace only over the momentum degrees of freedom, so  $\mathcal{G}_{jl}$  is a four by four matrix for each pair of lattice points  $j$  and  $l$ , where  $\tilde{\Lambda}(\mathbf{x}) = (\phi_c(|\mathbf{x}|)\delta_{\sigma\alpha}, b\phi_{\sigma\alpha}^6(\mathbf{x}) + b\phi_{\sigma\alpha}^7(\mathbf{x})(\hat{\mathbf{n}} \cdot \vec{\sigma}))$ .

The final spectral function is then

$$A(\mathbf{x}, \omega) = \frac{1}{\pi} \text{Im} \text{Tr} \left[ \sum_{j,l} \tilde{\Lambda}(\mathbf{x} - \mathbf{R}_j) \cdot \mathcal{G}_{jl}(\omega - i\delta) \cdot \tilde{\Lambda}^\dagger(\mathbf{x} - \mathbf{R}_l) \right] \quad (62)$$

To evaluate this quantity, the summations were limited to the four nearest neighbor sites at the corner of a plaquette. The positions  $\mathbf{x}$  were taken to lie in the plane of the  $U$  atoms. The wavefunctions  $\phi^6(|\mathbf{x}|) = e^{-|\mathbf{x}|/a}$ ,  $\phi^7(|\mathbf{x}|) = e^{-|\mathbf{x}|/a}$  and  $\phi_c(|\mathbf{x}|) = e^{-|\mathbf{x}|/a}$  were each taken to be simple exponentials of characteristic range equal to the  $U - U$  spacing  $a$ .

The nematicity of the tunneling conductance was then calculated numerically from the spatial integral

$$\eta(eV) = \frac{\int A(\mathbf{x}, eV) \text{sgn}(xy) dx dy}{\left( \int dx dy A(\mathbf{x}, eV)^2 - [\int dx dy A(\mathbf{x}, eV)]^2 \right)^{1/2}} \quad (63)$$

- 
- [1] H. Okhuni et al., “Fermi surface properties and de Haas-van Alphen oscillation in both the normal and superconducting mixed states of  $URu_2Si_2$ ”, *Philos. Mag. B* **79**, 1045 (1999).
- [2] A. F. Santander-Syro et al., “Fermi-surface instability at the ‘hidden order’ transition of  $URu_2Si_2$ ” *Nature Physics* **5**, 637 - 641 (2009).
- [3] P. M. Oppeneer, J. Ruzs, S. Elgazzar, M.-T. Suzuki, T. Durakiewicz, and J. A. Mydosh *Phys. Rev. B* **82**, 205103 (2010).
- [4] P. Haen, F. Lapiere, P. Lejay, J. Voiron, *J. Magnetism and Magnetic Materials* **116**, 108-110 (1992).
- [5] K. Haule and G. Kotliar, “Arrested Kondo Effect and Hidden Order in  $URu_2Si_2$ ,” *Nature Phys.* **5**, 796 (2009).
- [6] R. Okazaki et al., “Rotational Symmetry Breaking in the Hidden Order Phase of  $URu_2Si_2$ ”, *Science* **331** 439 (2011).
- [7] T.T.M. Palstra et al., “Superconducting and Magnetic Transitions in the Heavy-Fermion System  $URu_2Si_2$ ,” *Phys. Rev. Lett.* **55** 2727 (1985).
- [8] M. Jaime, K. H. Kim, G. Jorge, S. McCall, and J. A. Mydosh, “High Magnetic Field Studies of the Hidden Order Transition in  $URu_2Si_2$ ,” *Phys. Rev. Lett.* **89**, 287201 (2002).
- [9] E. A. Goremychkin, R. Osborn, B. D. Rainford, and A. P. Murani, “Evidence for Anisotropic Kondo Behavior in  $Ce_{0.8}La_{0.2}Al_3$ ,” *Phys. Rev. Lett.* **84**, 2211 (2000).
- [10] A. P. Ramirez, P. Coleman, P. Chandra, E. Brück, A. A. Menovsky, Z. Fisk, and E. Bucher, “Nonlinear susceptibility as a probe of tensor spin order in  $URu_2Si_2$ ”, *Phys. Rev. Lett.* **68**, 2680 (1992).
- [11] P. Chandra et al., *Physica B*, **199 & 200** 426 (1994).
- [12] A. Villaume et al., “Signature of Hidden Order in Heavy Fermion Superconductor  $URu_2Si_2$ : Resonance at the wave vector  $Q_0 = (1, 0, 0)$ ,” *Phys. Rev. B* **78** 5114 (2008).
- [13] C. Broholm et al., “Magnetic excitations in the heavy-fermion superconductor  $URu_2Si_2$ ,” *Phys. Rev. B* **43**, 12809 (1991).
- [14] M.B. Walter et al., “Nature of the order parameter in the Heavy-Fermion system  $URu_2Si_2$ ,” *Phys. Rev. Lett.* **71**, 2630 (1993).
- [15] S. Takagi et al., “No Evidence for “Small-Moment Antiferromagnetism” under Ambient Pres-

- sure in URu<sub>2</sub>Si<sub>2</sub> : Single-Crystal <sup>29</sup>Si NMR Study,” J. Phys. Soc. Jpn. 76, 033708 (2007).
- [16] H. Ikeda and K. Miyake, “A Theory of Anisotropic Semiconductor of Heavy Fermions,” J. Phys. Soc. Jpn. 65, 1769 (1996).
- [17] A.E. Sikkema, W.J.L. Buyers, I. Affleck and J.Gan, “Ising-Kondo lattice with transverse field: A possible f-moment Hamiltonian for URu<sub>2</sub>Si<sub>2</sub> ,” *Phys. Rev. B* **54**, 9322 (1996). ”
- [18] N. Kanchanavavatee et al, “Twofold enhancement of the hidden-order/large-moment antiferromagnetic phase boundary in the URu<sub>2</sub>xFexSi<sub>2</sub> system”, *Phys. Rev. B* 84, 245122 (2011).